

Static and dynamic functional connectomes represent largely similar information

Andraž Matkovič^{a,*}, Alan Anticevic^{b,c}, John D. Murray^{b,c,d}, Grega Repovš^a

^a*Department of Psychology, Faculty of Arts, University of Ljubljana,*

^b*Department of Psychiatry, Yale University School of Medicine, New Haven, United States,*

^c*Interdepartmental Neuroscience Program, Yale University, New Haven, United States,*

^d*Department of Psychiatry, Yale University, New Haven, United States,*

Abstract

Functional connectivity (FC) in blood oxygen level-dependent (BOLD) fMRI time series can be estimated using methods that differ in sensitivity to the temporal order of time points (static vs. dynamic) and the number of regions considered in estimating a single edge (bivariate vs. multivariate). Previous research suggests that dynamic FC explains variability in FC fluctuations and behavior beyond static FC. Our aim was to systematically compare methods on both dimensions. We compared five FC methods: Pearson's/full correlation (static, bivariate), lagged correlation (dynamic, bivariate), partial correlation (static, multivariate) and multivariate AR model with and without self-connections (dynamic, multivariate). We compared these methods (i) directly, by assessing the similarities between the FC matrices, and (ii) indirectly, by comparing the patterns of brain-behavior associations. Although FC estimates did not differ as a function of sensitivity to temporal order, we observed differences between the multivariate and bivariate FC methods. The dynamic FC estimates were highly correlated with the static FC estimates, especially when comparing group-level FC matrices. Similarly, there were high correlations between the patterns of brain-behavior associations obtained using the dynamic and static FC methods. We conclude that the dynamic FC estimates represent information largely similar to that of the static FC.

Keywords: functional connectivity, autoregressive model, dynamic functional connectivity, brain-behavior associations

1. Introduction

Brain functional connectivity (FC) is estimated by calculating statistical associations between time series of brain signal [1], which reflect functional relationships between brain regions [2]. The investigation of FC has improved our understanding of brain function in health and disease and has been shown to be useful as a tool to predict interindividual differences, such as cognition, personality, or the presence of mental or neurological disorders [3, 4]. In functional magnetic resonance imaging (fMRI) studies, FC is most commonly estimated using the Pearson's correlation coefficient between time series of pairs of regions. Although correlation is simple to understand and compute, it is insensitive to the temporal order of time points. Measures or models that are sensitive to the temporal order of time points are called *dynamic*, while measures that are insensitive to temporal order are measures of *static* FC. Given that the information flow in the brain is causally organized in time [5, 6], dynamic connectivity models could be more informative in terms of understanding brain function and investigating brain-behavior associations.

Dynamic FC can be estimated using measures of lag-based connectivity, such as lagged correlation or multivariate autoregressive (AR) model. In contrast to static FC, dynamic FC methods can be used to estimate the *directionality* of information flow based on temporal precedence [7]. Although these methods have been commonly used, some studies [7, 8, 9, 10, 11] have warned that the ability of these methods to accurately estimate the presence and directionality of connections is compromised due to the convolution of the neural signal with the hemodynamic response function

*Corresponding author

Email address: andraz.matkovic@ff.uni-lj.si (Andraž Matkovič)

19
17 (HRF) and the resulting blurring of the signal, due to interregional variability of HRF, noise [7, 8, 9, 10], and/or
18 downsampling of the neural signal in fMRI [11]. Other studies [12, 13, 14] have shown that the measures of dynamic
20 FC complement the measures of static FC. For example, lagged FC measures can improve discrimination between
21 individuals and between tasks [12, 13] and can be used to improve effective connectivity estimates [14]. Furthermore,
22 Liégeois et al. [15] have shown that the multivariate AR model explains temporal FC fluctuations better than Pearson's
23 correlations.

24 In subsequent research Liégeois et al. [16] showed that static FC and dynamic FC exhibit different patterns of
25 brain-behavior associations. They concluded that dynamic FC explains additional variance in behavior beyond vari-
26 ance that can be explained by static FC. However, this comparison confounds two orthogonal properties of FC meth-
27 ods. Although Pearson's correlation and multivariate AR models differ in their sensitivity to temporal reordering (i.e.,
28 static vs. dynamic), they also differ in terms of how many variables (brain regions) are taken into account during the
29 estimation of a single edge (bivariate vs. multivariate). Hence, a more valid comparison between static and dynamic
30 FC methods should consider both dimensions: the number of variables and the sensitivity to temporal reordering.
31 Combining these two factors enables us to differentiate between four basic classes of FC methods (see Figure 1).

32 Our aim was to systematically compare the FC estimated by both dimensions, that is, the sensitivity to temporal
33 reordering (static vs. dynamic) and the number of independent variables (bivariate vs. multivariate). We focused on
34 five mathematically related methods: full/Pearson's correlation, partial correlation, lagged correlation, and multivariate
35 AR model with and without self-connections, where self-connections refer to autocorrelation of the region with
36 itself [17, 18]. We were interested in similarities of the FC estimates and patterns of brain-behavior associations.
37 We compared FC methods (i) directly by assessing similarities between FC matrices and (ii) indirectly by comparing
38 brain-behavior associations. In addition, to better understand the results obtained using different methods and the
39 relationship between them, we generated and analyzed synthetic data in which we systematically varied the length of
40 time series and the amount of noise.

41 We used empirical and simulated data to test two hypotheses. First, we predicted that dynamic and static FC
42 methods will provide similar FC estimates due to autocorrelation of the fMRI time series. Autocorrelation is inherent
43 to the fMRI signal and originates from two main sources: physiological noise and convolution of neural activity with
44 HRF [19]. We expected that the degree of similarity between static and dynamic FC estimates would be similar to
45 or larger than the average autocorrelation of the fMRI time series. Furthermore, we expected the similarity between
46 dynamic and static FC to be smaller when the fMRI time series is pre-whitened (i.e., when autocorrelation is removed
47 before computation of FC).

48 Second, we predicted that multivariate methods can improve inferences about causal relationships between re-
49 gions, as they estimate *direct* connections by removing the confounding influence of indirect associations [2] as
50 opposed to bivariate methods, which cannot separate *indirect* and *direct* connections [18]. By providing more direct
51 information on causal relationships between brain regions [20], multivariate methods could improve brain-behavior
52 associations in terms of explained variance and/or brain-behavior correlation estimates. Existing research has shown
53 inconsistent differences in behavior predictive accuracy between partial and full/Pearson's correlations, favoring either
54 partial [21, 22] or full correlation [23] or showing negligible differences between them [24].

55 2. Method

56 2.1. Participants

57 To address the research questions, the analyzes were performed on publicly available deidentified data from 1096
58 participants ($M_{age} = 28.8$, $SD_{age} = 3.7$, 596 women) included in the Human Connectome Project, 1200 Subjects
59 Release [25]. Each participant took part in two imaging sessions over two consecutive days that included the acqui-
60 sition of structural, functional (rest and task), and diffusion-weighted MR images. The study was approved by the
61 Washington University institutional review board and informed consent was signed by each participant.

62 2.2. fMRI data acquisition and preprocessing

63 Data were acquired in two sessions using the Siemens 3T Connectome Skyra tomograph. Structural MPRAGE
64 T1w image (TR = 2400 ms, TE = 2.14 ms, TI = 1000 ms, voxel size = 0.7 mm isotropic, SENSE factor = 2, flip angle

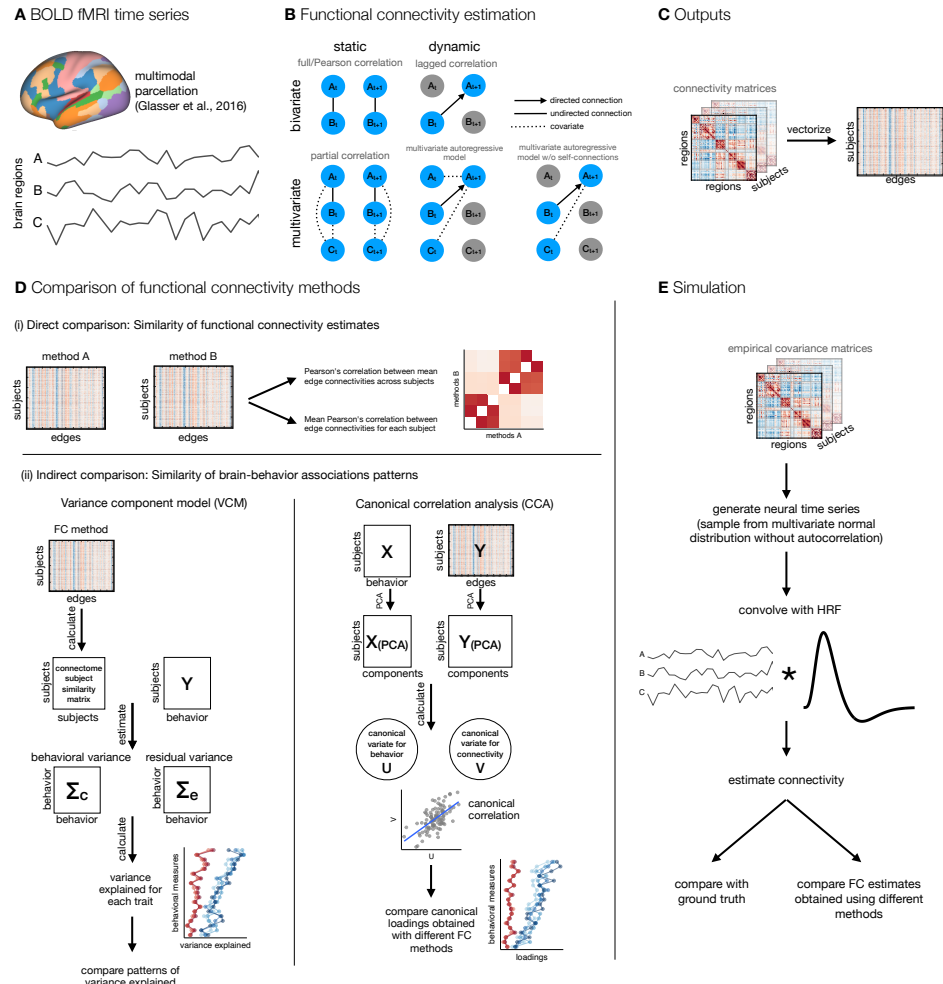


Figure 1: A schematic of analysis steps. **A.** BOLD fMRI data was preprocessed, parcellated, and individual parcel timeseries were extracted. **B.** Functional connectivity (FC) was estimated with five methods that differed along two dimensions: static vs. dynamic and bivariate vs. multivariate. Static FC refers to measures that are insensitive to temporal order and can be estimated using full/Pearson's correlation or partial correlation, whereas measures of dynamic FC are sensitive to temporal order of time points. Dynamic FC can be estimated using measures of lag-based connectivity, such as lagged correlation, or using the linear multivariate autoregressive (AR) model. The lagged correlation between two time series is calculated by shifting one time series by p time points. Similarly, a p -th order multivariate (or vector) autoregressive model predicts the activity of a particular brain region at time point t based on the activity of all regions at time point(s) from $t - p$ to $t - 1$. Bivariate and multivariate FC methods differ in terms of number of variables (regions) taken into account when estimating connectivity at a single edge: bivariate connectivity between two regions depends only on the two regions, whereas multivariate connectivity between two regions includes all other regions as covariates. **C.** FC matrices were vectorized. **D.** FC estimates were compared both (i) directly by calculating correlations between FC estimates and (ii) indirectly by comparing estimates of brain-behavior associations across FC methods. **E.** Additionally, we performed simulation to assess the influence of random noise and signal length on the similarity between FC estimates obtained using different methods.

65 = 8°) and T2w image (TR = 3200 ms, TE = 565 ms, voxel size = 0.7 mm isotropic) were acquired in the first session.
66 The participants underwent four resting state fMRI runs, two in each session (gradient echo EPI sequence, multiband
67 factor: 8, acquisition time: 14 min 24 s, TR = 720 ms, TE = 33.1 ms, flip angle = 52°).

68 Initial preprocessing was performed by the HCP team and included minimal preprocessing [26], ICA-FIX denoising
69 [27] and MSMAll registration [28]. The data was then further processed using QuNex [29] to prepare them for
70 functional connectivity analyzes. First, we identified frames with excessive movement and/or frame-to-frame signal
71 changes. We marked any frame that was characterized by frame displacement greater than 0.3 mm or for which the
72 frame-to-frame change in signal, computed as intensity normalized root mean squared difference (DVARs) across all
73 voxels, exceeded 1.2 times the DVARs median across the time series, as well as one frame before and two frames
74 after them. Marked frames were used for motion censoring, which is described in detail in the Appendix. Next, we
75 used linear regression to remove multiple nuisance signals, including six movement correction parameters and their
76 squared values, signals from the ventricles, white matter and the whole brain, as well as the first derivatives of the
77 listed signals. The previously marked frames were excluded from the regression and all subsequent analysis steps were
78 performed on the residual signal. No temporal filtering was applied to the data, except a very gentle high-pass filter at
79 the cutoff of 2000 s applied by the HCP team [26], since temporal filtering could introduce additional autocorrelation
80 [30] and inflate correlation estimates [19, 31].

81 Only sessions with at least 50% useful frames after motion censoring were used in the further analysis, except
82 where noted otherwise. This resulted in 1003 participants with at least one session. Before FC analyzes, all resting-
83 state BOLD runs from available sessions were concatenated and parcellated using a multimodal cortical parcellation
84 (MMP1.0) containing 360 regions [28]. Each parcel was represented by a mean signal across all the parcel grayordi-
85 nates.

86 2.3. Functional connectivity estimation

87 Functional connectivity was estimated using five methods: full (Pearson's) correlation, partial correlation, lagged
88 correlation, multivariate AR model (also called vector AR model), and multivariate AR model without self-connections.
89 The listed methods differ in terms of the number of regions used to estimate the connectivity of a single edge (bivariate
90 vs. multivariate) and in terms of sensitivity to temporal reordering of time points (static vs. dynamic) (see Figure 1).
91 A multivariate AR model without self-connections was included to test how much similarity between the multivariate
92 AR model and partial correlation depends on self-connections (the diagonal terms in the autocovariance matrix).

93 The bivariate static FC was estimated using full correlation. Let x_i be a demeaned $T \times 1$ vector of region i time
94 series (T is the number of time points) and let $X = [x_1, \dots, x_N]'$ be a $N \times T$ matrix of the demeaned region time series
95 (N is the number of regions). Then the sample covariance matrix C can be estimated with

$$C = \frac{XX'}{T - 1} \quad (1)$$

96 A correlation matrix can be obtained by standardizing the time series to zero mean and unit standard deviation
97 (i.e., z -scores) beforehand.

98 Multivariate static FC was estimated using partial correlation. Partial correlations were computed by taking an
99 inverse of a covariance matrix (i.e., the precision matrix) and then standardizing and sign-flipping according to the
100 equation:

$$\rho_{ij} = -\frac{w_{ij}}{\sqrt{w_{ii}w_{jj}}} \quad (2)$$

101 where ρ is an element of a partial correlation matrix, w is an element of a precision matrix, and i and j are the indices
102 of rows and columns, respectively [32].

103 Dynamic bivariate connectivity was estimated using lagged correlation (also known as autocovariance matrix).
104 Autocovariance is defined as the covariance of time series with lagged time series. Let X_t be an $N \times (T - p)$ matrix
105 of shortened time series with time points from 1 to $T - p$ (p is the lag/model order) and X_{t+p} be a similar matrix with
106 time points from $p + 1$ to T . Then,

$$C_p = \frac{X_{t+p}X_t'}{T - p} \quad (3)$$

107 is p -th order autocovariance or lagged covariance matrix. Diagonal entries are called autocovariances or, some-
108 times, self-connections or self-loops [18, 17]. Off-diagonal entries of autocovariance matrix are also called cross-
109 covariances. Note that the autocovariance matrix of lag 0 is equal to the ordinary covariance matrix. The autocorrela-
110 tion matrix was obtained by standardizing time series before computing autocovariance.

111 Correlations, autocorrelations, and partial correlations were Fisher z -transformed for subsequent analyzes.

112 Multivariate dynamic connectivity was estimated using the Gaussian multivariate AR model. Let Z be an $Np \times$
113 $(T - p)$ matrix of stacked matrices of shortened time series, $Z = [X'_{t+p-1}, \dots, X'_{t+1}, X'_t]'$. The multivariate AR model
114 can be written in matrix notation as:

$$X_{t+p} = AZ + E \quad (4)$$

115 where A is an $N \times Np$ matrix of AR coefficients of the p -th order model and E is an $N \times (T - p)$ matrix of zero-mean,
116 independent, normally distributed residuals. The matrix A can be estimated using the ordinary least squares (OLS)
117 estimator:

$$\hat{A} = X_{t+p}Z'(ZZ')^{-1} \quad (5)$$

118 For $p = 1$ \hat{A} equals:

$$\hat{A} = X_{t+p}X'_t(X_tX'_t)^{-1} \quad (6)$$

119 The equation shows that the coefficients of the multivariate AR model are a product of the lagged covariance and
120 (non-lagged) precision matrix. Therefore, the multivariate AR model encodes both static and dynamic FC. The same
121 can be inferred from the Yule-Walker equations (see Liégeois et al. [15], Chatfield and Xing [33]). Moreover, for lag
122 0, the multivariate coefficients of the AR model are equal to the covariance matrix (see [15]).

123 To estimate the coefficients of the multivariate AR model without self-connections, we fitted the model

$$x_{i,t+p} = X'_t a_i + e_i \quad (7)$$

124 for each region i separately, such that we set i -th row of matrix X_t to zero (the equation above applies for $p = 1$ only, but
125 the model could be extended to include higher lags as in Equation 4). Vectors $x_{i,t+p}$ were taken from rows of the matrix
126 X_{t+p} and included time points from $p + 1$ to T . Vectors e_i represent normally distributed, zero-mean, independent
127 residuals. FC matrix was constructed by organizing $N \times 1$ vectors a_i into the $N \times N$ matrix $A_1 = [a_1, \dots, a_N]'$. This
128 matrix is asymmetric with zeros on the diagonal. The coefficients of both multivariate AR models were estimated
129 using the coordinate descent algorithm implemented in the GLMnet package for MATLAB [34].

130 All AR models were estimated for lag 1 only. This order was shown to be optimal for the multivariate AR model
131 for resting state fMRI data with a high number of regions [35, 36], and also in a study using HCP data [37]. There were
132 no differences between the variance of order 1 and the higher-order models explained by the first principal component
133 of the null data generated from the multivariate AR model in a previous study [15]; therefore, we did not consider
134 higher-order autoregressive models.

135 2.4. Prewhitening

136 We expected that FC estimates based on AR models would be similar to static FC estimates due to autocorrelation
137 present in the fMRI time series. To test the similarity between static and dynamic FC in the absence of autocorrelation,
138 we computed connectivity both from non-prewhitened time series and on prewhitened time series. The exception was
139 multivariate AR model, where the diagonal term (self-connections) effectively acts as a prewhitening. The difference
140 between the multivariate AR model with and without prewhitening is essentially the difference between the multivari-
141 ate AR model with and without self-connections. We performed prewhitening by taking the residuals of the regression
142 of the "raw" time series on lagged time series.

143 To retain frame sequence after prewhitening, frames that were marked as bad in any of the original or lagged time
144 series were set to zero before computing residuals. For this reason, frames that were preceded by a bad frame in any
145 of the 1 to l previous frames were not prewhitened. At higher orders, this resulted in fewer total prewhitened frames.

146 Prewhitening was performed on orders 1 to 3 (abbreviated AR1/2/3 prewhitened). Autocorrelations were already
147 significantly reduced at order 1 and were additionally reduced at lags 2 and 3 (Figure S1). Since the results were

148 similar regardless of the prewhitening order, only the results for the prewhitening on order 1 are shown in the main
149 text, and the results for higher orders are shown in the supplement.

150 2.5. Similarities between FC estimates obtained using different methods

151 We estimated similarities between the FC estimates by computing the correlation between vectorized FC matrices.
152 We adjusted the vectorization for each pair of methods so that only unique elements were taken into account. For
153 example, correlation and partial correlation matrices are symmetric; therefore, only the upper or lower triangular part
154 of the matrix (without the diagonal) should be considered. On the other hand, the FC matrices derived from the
155 AR models are not symmetric; therefore, the whole matrix must be vectorized. The exception is the multivariate
156 AR model without self-connections, which does not contain any information on the diagonal, so in this case matrix
157 without the diagonal needs to be vectorized. When comparing asymmetric and symmetric matrices, we computed and
158 used the average of the upper and lower triangular parts of the matrix (using equation $(X + X')/2$).

159 We estimated similarities in two ways: first, by computing correlations between connectivity estimates for each
160 subject separately and then averaging the resulting correlations (mean correlations between individual-level FC ma-
161 trices), and second, by averaging FC matrices over participants and then computing correlation between methods on
162 group FC matrices (correlations between group-level FC matrices).

163 To test how similarity between FC estimates depends on data quality, we repeated analyses on a subset of 200
164 participants with the largest number of retained frames.

165 2.5.1. Correlation between edge similarity and test-retest reliability

166 To better understand the origin of the similarities between the FC methods, we examined the relationship between
167 the edge similarity of the FC estimates obtained using different methods and test-retest reliability at the edge level. If
168 similarities between FC estimates depend on the signal-to-noise ratio (SNR), more reliable edges will be more similar
169 across methods.

170 We computed the edge similarity as correlation at every edge for each pair of FC methods. We estimated the
171 test-retest reliability using the intraclass coefficient (ICC) for each method separately. We estimated the variance
172 components within the linear mixed model framework using the restricted maximum likelihood (REML) procedure
173 [38, 39]. We defined variance components as follows:

$$\text{var}(y_{pdr}) = \sigma_p^2 + \sigma_d^2 + \sigma_r^2 + \sigma_{p \times r}^2 + \sigma_{p \times d}^2 + \sigma_{d \times r}^2 + \sigma_e^2 \quad (8)$$

174 where y is an estimate of an edge, p indicates participant, d day, r run and e residual.

175 We computed the ICC as a ratio between between-subject variance (which included interaction terms pertaining
176 to participants) and the total variance [40]. For this analysis, the runs were not concatenated.

177 Finally, we applied Fisher's z -transformation to both edge similarity and ICC and computed the correlation be-
178 tween them. To reduce the number of comparisons, we only investigated the most relevant comparisons: full cor-
179 relation vs. lagged correlation, partial correlation vs. multivariate AR1, and partial correlation vs. multivariate AR1
180 without self-connections. Since we estimated test-retest reliability separately for each method in a pair, there were
181 two correlations for each pair of methods. We averaged both correlations for each comparison.

182 2.6. Brain-behavior associations

183 To compare the brain-behavior associations obtained by different FC measures, we used 58 behavioral measures
184 (see Table S1) that included cognitive, emotion and personality measures and were previously used in other studies
185 [16, 41, 42].

186 2.6.1. Variance component model

187 We computed brain-behavior associations using the multivariate variance component model (VCM), developed by
188 Ge et al. [43] to estimate heritability. The use of the variance component model to estimate associations between the
189 brain and behavior was introduced by Liégeois et al. [16]. We adopted the same approach to allow direct comparison
190 with the results reported by Liégeois et al. [16]. Furthermore, the use of VCM allows an easy calculation of the
191 explained variance for single traits. The model has the form

$$Y = C + E \quad (9)$$

192 where Y represents the $N \times P$ matrix (number of subjects \times number of traits) of behavioral measures, C represents
193 shared effects and E represents unique effects. The model has the following assumptions:

$$\begin{aligned} \text{Vec}(C) &\sim \mathcal{N}(\Sigma_c \otimes F) \\ \text{Vec}(E) &\sim \mathcal{N}(\Sigma_e \otimes I) \end{aligned} \quad (10)$$

194 where $\text{Vec}(\cdot)$ is the matrix vectorization operator, \otimes is the Kronecker product operator, and I is the identity matrix.
195 F represents $N \times N$ matrix of similarities between participants, which were estimated with the Pearson's correlation
196 coefficient. Σ_c and Σ_e are $P \times P$ matrices, which are being estimated. The total variance explained is computed as:

$$M = \frac{\text{Tr}(\Sigma_c)}{\text{Tr}(\Sigma_c) + \text{Tr}(\Sigma_e)} \quad (11)$$

197 where $\text{Tr}(\cdot)$ represents the trace operator, and:

$$M_i = \frac{\Sigma_c(i, i)}{\Sigma_c(i, i) + \Sigma_e(i, i)} \quad (12)$$

198 for single traits. M is analogous to the concept of heritability and can be interpreted as the amount of variance in
199 behavior that can be explained with the variance in the connectome.

200 Before computing VCM, we imputed missing behavioral data using the R package `missForest` [44]. There were
201 0.59% missing data points overall. Following the procedure of Liégeois et al. [16], we applied quantile normalization
202 to behavioral data. To remove potential confounding factors, we regressed age, gender, race, education, and movement
203 (mean FD) using the procedure described in Ge et al. [45, 43].

204 We estimated M for each connectivity method separately. We compared patterns of explained variances by corre-
205 lating the variance explained at the trait level between all methods.

206 Since the results of VCM are based on similarities between participants (matrix F), we tested the extent to which
207 the similarities between participants, and thus the results of VCM, depend on the levels of noise in the data. To this
208 end, we performed a simulation in which we added random Gaussian noise (mean 0, standard deviation 0–1 in steps
209 of 0.1) to the standardized time series. To reduce complexity, we performed this analysis only for static FC methods.

210 2.6.2. Canonical correlation analysis

211 Since VCM is rarely used to study brain-behavior associations, we repeated the analysis using canonical cor-
212 relation (CCA). CCA is used to reveal the low-dimensional structure of the shared variability between two sets of
213 variables (in our case, connectivity and behavior).

214 Let X and Y be $N \times P$ and $N \times Q$ matrices (N is the number of observations, P and Q are the number of variables),
215 respectively. CCA aims to find a solution to the following set of equations:

$$\begin{aligned} U &= XA \\ V &= YB \end{aligned} \quad (13)$$

216 where $U_{N \times K}$ and $V_{N \times K}$ are matrices of canonical scores (or variables) and $A_{P \times K}$ and $B_{Q \times K}$ are matrices of canonical
217 weights. The solution to the above set of equations is found under the constraint $U'U = V'V = I$. The columns of
218 the U and V matrices tell us the relative position of each observation in the canonical variables. In contrast, columns
219 of the A and B matrices contain information on the relative contribution of each variable to each of the canonical
220 variables. Canonical correlations are correlations between columns of U and V . Additionally, one can calculate
221 canonical loadings - the correlations between original data matrices and canonical scores. Canonical variables are
222 ordered in descending order according to the size of canonical correlations. Usually, only the first or first few canonical
223 components are of interest, as these explain most of the shared variance. Mathematical details on CCA can be found
224 elsewhere [e.g. 46, 47, 48, 49, 50].

225 We performed the CCA using the GEMMR package [47]. To prepare the data for CCA, we followed the procedure
226 by Smith et al. [51], including deconfounding using the same variables as for VCM. Prior to CCA, we reduced the
227 dimensionality of both sets of variables to 20 components using principal component analysis (PCA). This number
228 was chosen to optimize the number of samples per feature based on the recommendation by Helmer et al. [47] under
229 the assumption of a real first canonical correlation $r = .30$. We performed a 5-fold cross-validation to assess the
230 generalizability of the model. We only examined the first canonical correlation since it was shown that the first
231 canonical variable explains the most shared variance, and it was the only statistically significant canonical variable in
232 a previous study [51].

233 We repeated the CCA for all FC methods. The similarities between the methods were assessed by comparing
234 the first canonical correlation obtained in the training and the test set. Next, we correlated the canonical weights and
235 loadings related to behavior.

236 2.6.3. Control analyses

237 Participants in the HCP dataset are genetically and environmentally related, which can inflate between-subject
238 similarities and influence the results related to interindividual differences. Therefore, we repeated all analyses related
239 to brain-behavior associations on two subsamples of genetically unrelated participants (sample sizes 384 and 339).

240 2.7. Simulation

241 We hypothesized that dynamic and static FC estimates would be similar due to autocorrelation of fMRI time
242 series, which is partly the result of convolution of neural time series with HRF. In addition, an important source of
243 similarities (or differences) between FC results obtained by different methods could be due to similar (or different)
244 effects of the amount of noise and the amount of available data on the resulting FC matrices. To evaluate the impact of
245 convolution with HRF, signal quality, and the amount of data on estimated similarities between results using different
246 FC measures, we used numerical simulations of data with known covariance structure. We generated multivariate time
247 series of events for 1000 "participants." Events were sampled from a multivariate normal distribution with a mean of
248 zero. The covariances differed for each participant and were taken from experimental data parcellated using Schaefer's
249 local-global parcellation with 100 regions [52]. We used this parcellation instead of MMP to reduce the computational
250 burden and the size of the generated data. Events were not autocorrelated. The generated events were then convolved
251 with HRF using the SimTB toolbox [53]. TR was set to 0.72 s (the same as in HCP data), and HRF parameters were
252 set equal for all participants and regions (delay of response: 6, delay of the undershoot: 15, dispersion of the response:
253 1, dispersion of the undershoot: 1, the ratio of response to the undershoot: 3, onset in seconds: 0, length of the kernel
254 in seconds: 32). The resulting time series were standardized.

255 To estimate the effects of signal quality on FC estimates and on similarities between FC methods, we added
256 Gaussian noise with zero mean and standard deviation ranging from 0 to 1 standard deviation in steps of 0.1. This
257 translates to SNR from 10 to 1 (excluding time series without noise, which has infinite SNR). We varied the time-series
258 durations from 500 to 10000 data points in steps of 500.

259 The first step in the analysis was to establish the ground truth for each method, that is, the results that would be
260 obtained in an ideal situation. We defined the ground truth as FC at maximum length and without noise in the event
261 time series. Note that because events were not autocorrelated, the ground truth for all autoregressive FC methods was
262 a matrix with all zero entries.

263 Next, we compared results using different FC methods in the same manner as for experimental data for all noise
264 level and signal length combinations on prewhitened and non-prewhitened data. We computed (1) correlations be-
265 tween ground truth FC matrices and simulated FC matrices for all FC methods and (2) correlations between FC esti-
266 mates obtained using different methods. To reduce the number of comparisons, we only investigated the most relevant
267 comparisons: full correlation vs. lagged correlation, partial correlation vs. multivariate AR, and partial correlation vs.
268 multivariate AR without self-connections.

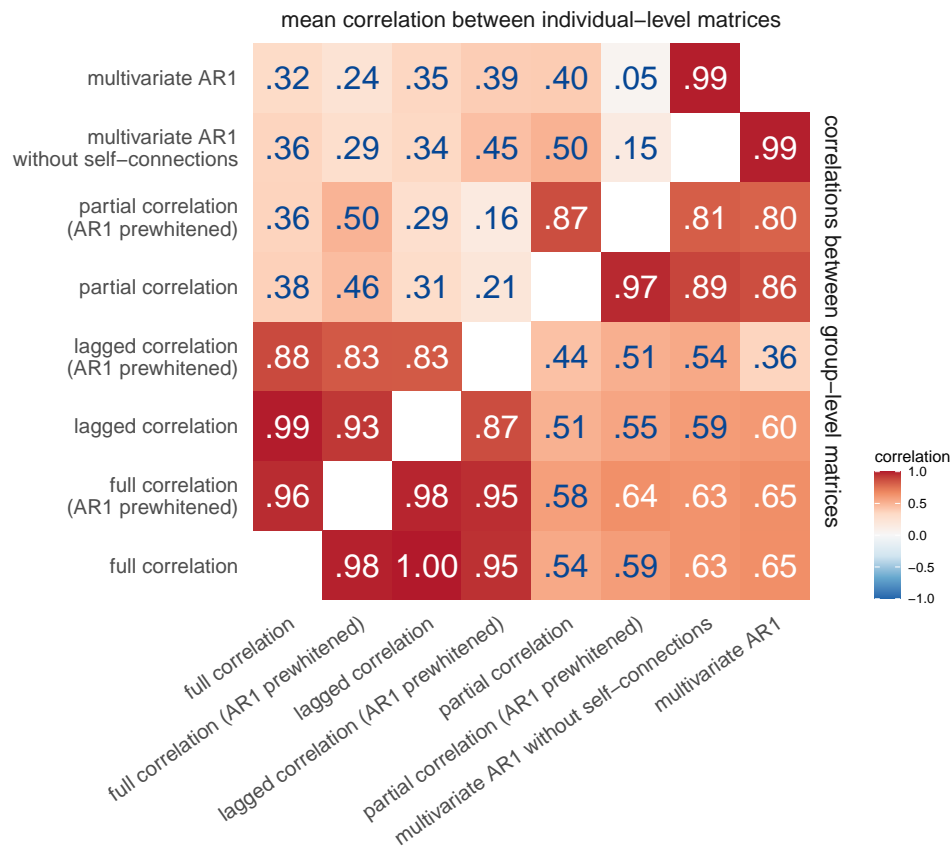


Figure 2: Correlations between FC estimates obtained using different FC methods. We calculated the similarities between FC estimates obtained using different FC methods (i) by averaging connectivity matrices across participants and then computing correlations between them (correlation between group-level FC, bottom right triangle), and (ii) by computing correlations between the FC estimates for each participant separately and then averaging across participants (correlation between individual-level FC, top left triangle).

269 3. Results

270 3.1. Experimental data

271 3.1.1. Similarities between FC estimates obtained using different methods

272 To address our research questions, we first focused on estimating similarities between the results obtained with
273 different FC methods using empirical data. Comparison of group-level FC matrices showed very high correlations
274 between FC results obtained using bivariate methods ($r \geq .87$, Figure 2), as well as between results obtained using
275 multivariate methods (correlation between partial correlation [AR1 prewhitened] and multivariate AR model: $r = .80$).
276 In contrast, the correlations between the bivariate and multivariate FC estimates were lower and ranged from .36 to
277 .65.

278 When comparing and pooling results based on individual-level FC matrices, the mean correlation between FC
279 matrices obtained using different methods was lower. The correlations between the bivariate methods were still
280 very high (correlation between lagged and full correlation: $r = .99$, correlation between prewhitened lagged and
281 prewhitened full correlation: $r = .83$), while the correlations between the multivariate methods were lower on average.
282 In particular, the correlation between the partial correlation (AR1 prewhitened) and the multivariate AR model was
283 .05, compared to .80 between the group-level FC matrices.

284 The correlations between the results obtained using static and dynamic FC methods were smaller after prewhiten-
285 ing, with the greatest differences when comparing individual-level FC matrices obtained using multivariate methods.
286 Specifically, the correlation between the coefficients of the multivariate AR model and the partial correlation decreased
287 from .40 to .05 in the individual-level FC and from .86 to .80 in the group-level FC. The order of prewhitening had
288 minimal effect on the correlations between the methods (Figure S3), except for the comparison of the results obtained
289 using the multivariate AR model and the partial correlation at the individual-level FC, where the correlations increased
290 from .05 to .12 ($r = .15-.22$ for the multivariate AR model without self-connections).

291 The correlations between the FC results obtained using different methods were slightly higher when the analysis
292 was repeated on 200 participants with the highest data quality (Figure S4).

293 3.1.2. Correlation between edge similarity and test-retest reliability

294 We computed edge similarity between FC methods as a correlation over subjects at every edge for selected pairs
295 of FC methods. We estimated test-retest reliability at every edge for each method separately. Next, we computed the
296 correlation between edge similarity and test-retest reliability for each of selected pairs of FC methods. The correlation
297 was moderate to high for pairs of multivariate methods ($r = .47-.66$) and high for pairs of bivariate methods ($r = .55-
298 .79$, Figure 3)). Prewhitening lowered the correlations..

299 3.1.3. Brain-behavior associations estimated using variance component model

300 Next, we compared patterns of brain-behavior associations derived from different FC methods. The results of
301 the VCM show that bivariate methods explain about 30 percentage points less variance in behavior than multivariate
302 methods (Figure 4A,B). Furthermore, the similarity of patterns of variance explained over behavioral measures was
303 high between static and dynamic FC methods using the same number of variables, i.e., between full correlation and
304 lagged correlation ($r = 1.00$), and between partial correlation and multivariate AR models ($r = .83-.86$, Figure 4A,C).
305 The pattern of similarities in behavioral variance explained between the FC methods was comparable to the direct
306 comparison of the FC matrices (Figure 4C, cf. Figure 2). Patterns of similarities between the FC methods were similar
307 when the analysis was performed on subsamples of unrelated participants (Figure S5); however, the differences in total
308 variance explained between the bivariate and multivariate methods were smaller.

309 Simulation of the effects of noise in which we added various levels of noise to the fMRI time series showed that
310 noise affects estimates of the behavioral variance explained by the connectome. In particular, the mean of the variance
311 explained increased with increasing noise for both the full correlation and the partial correlation, but the increase was
312 more pronounced in the case of partial correlations (Figure 5B). This pattern was not equal for all behavioral variables
313 – for some, the variance explained decreased and for others, it increased (Figure 5A). On the other hand, the similarity
314 between the participants decreased with increasing noise (Figure 5C). This effect was more pronounced for partial
315 correlation compared to full correlation.

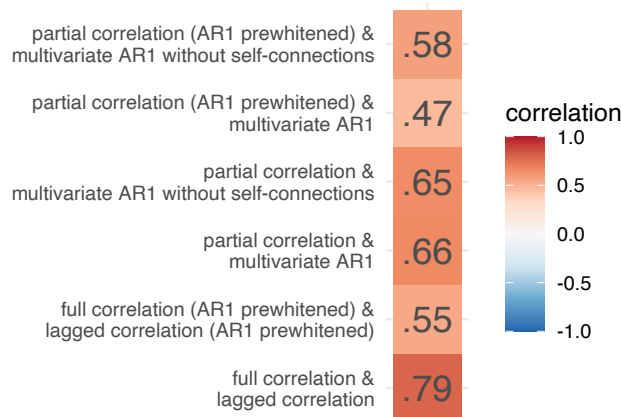


Figure 3: Correlations between edge similarity and test-retest reliability for selected pair of FC methods.

3.1.4. Brain-behavior associations estimated using canonical correlation analysis

The results of the similarity between the FC methods when investigating brain-behavior associations using CCA were comparable to those obtained using VCM. In particular, the correlations between the weights or loadings on behavioral measures between the FC methods were high when comparing the methods that use the same number of variables for the estimation of a single edge ($r > .80$) (Figure 6C). On the other hand, there was no discernible difference between dynamic and static FC estimates.

The first canonical correlation was around .70 in the training sample for the bivariate methods and around .50 for the multivariate methods (Figure 6B). Cross-validated R was much lower, around .40 for bivariate methods and around 0.05 for multivariate methods. Although these results differ from VCM (where multivariate methods explained more variance), the pattern of similarity between FC methods is the same.

The pattern of results was similar for the subsamples of unrelated participants, but the differences between the training and test sets were larger (Figure S6). The large difference between the performance of the model in training and test sets is indicative of overfitting, which is characteristic of CCA with a small number of samples per feature [47].

3.2. Evaluation of similarities between methods on simulated data

3.2.1. Relationship between FC estimates and ground truth

Correlations of FC estimates with ground truth were greater than 0.8 for full correlation and between 0.25 and 0.9 for partial correlation (Figure 7). Prewhitening decreased the correlation with ground truth. This effect was more pronounced for partial correlations. Longer time series also had higher correlations with ground truth (the difference was up to .5 for partial correlation and up to .3 for full correlation). The correlation with ground truth generally decreased with decreasing SNR (increasing noise), but in the case of partial correlation, these effects were not monotonic. In particular, for short time series, correlation with ground truth increased with low to moderate noise. Also in the case of partial correlation, prewhitening increased the correlation with ground truth at low noise. In contrast, prewhitening decreased the correlation with ground truth in the presence of high noise compared to the case without prewhitening.

3.2.2. Similarity between FC estimates

The connectivity matrices computed on the simulated data were compared in the same manner as for the experimental data. For brevity, we focus only on the three most relevant comparisons (lagged correlation vs. full correlation, multivariate AR model vs. partial correlation, multivariate AR model without self-connections vs. partial correlation).

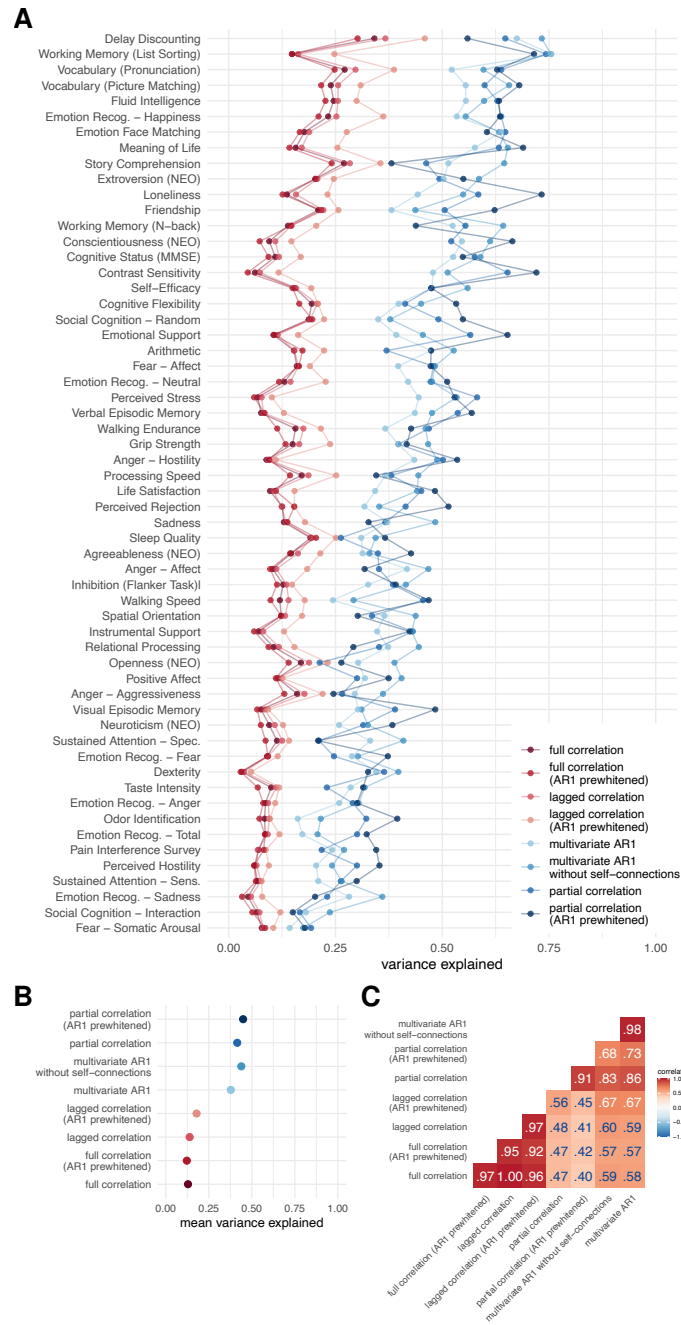


Figure 4: **Results of variance component model for brain-behavior associations.** **A.** Variance explained for individual traits estimated with different connectivity methods – traits are ordered according to the mean variance explained across connectivity methods. **B.** Mean variance explained. **C.** Similarities of explained variance patterns between connectivity methods.

345 Estimates based on lagged and full correlation were highly similar ($r \approx 1$ in the case without prewhitening) for all
 346 levels of noise and signal length (Figure 7). The correlation between FC estimates was reduced for prewhitened data,
 347 especially for low signal lengths (< 1000 frames).

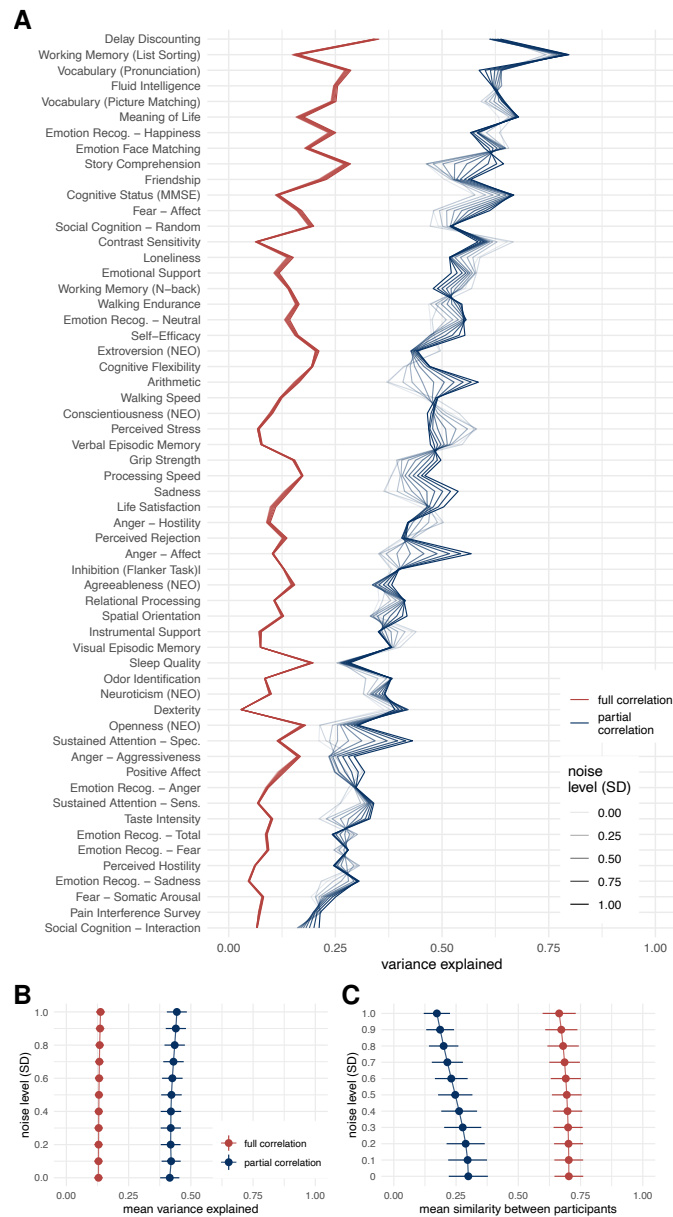


Figure 5: **Results of variance component model for brain-behavior associations on data with added noise.** FC was estimated using Pearson's/full correlation and partial correlation after adding various levels of random Gaussian noise to experimental time series. **A.** Variance explained for individual traits estimated with different connectivity methods. Traits are ordered according to the mean variance explained across connectivity methods. **B.** Mean variance explained. Error bars represent jackknife standard deviation. **C.** Mean similarity between participants. Error bars represent standard deviation.

348 The FC estimates of the multivariate AR model did not correlate with the FC estimates based on partial correlation
349 when the noise was low ($r = 0$ for zero noise). However, with increasing noise and increasing signal length, FC
350 estimates became very similar (up to $r = .95$), especially in the case without prewhitening and for long signal lengths.

351 Conversely, FC estimates based on a multivariate AR model without self-connections showed a high similarity
352 to the FC estimates based on partial correlation at a low noise level ($r > .95$). For prewhitened data, there was a
353 nonmonotonic relationship between FC estimates with increasing noise, but overall correlations remained high in

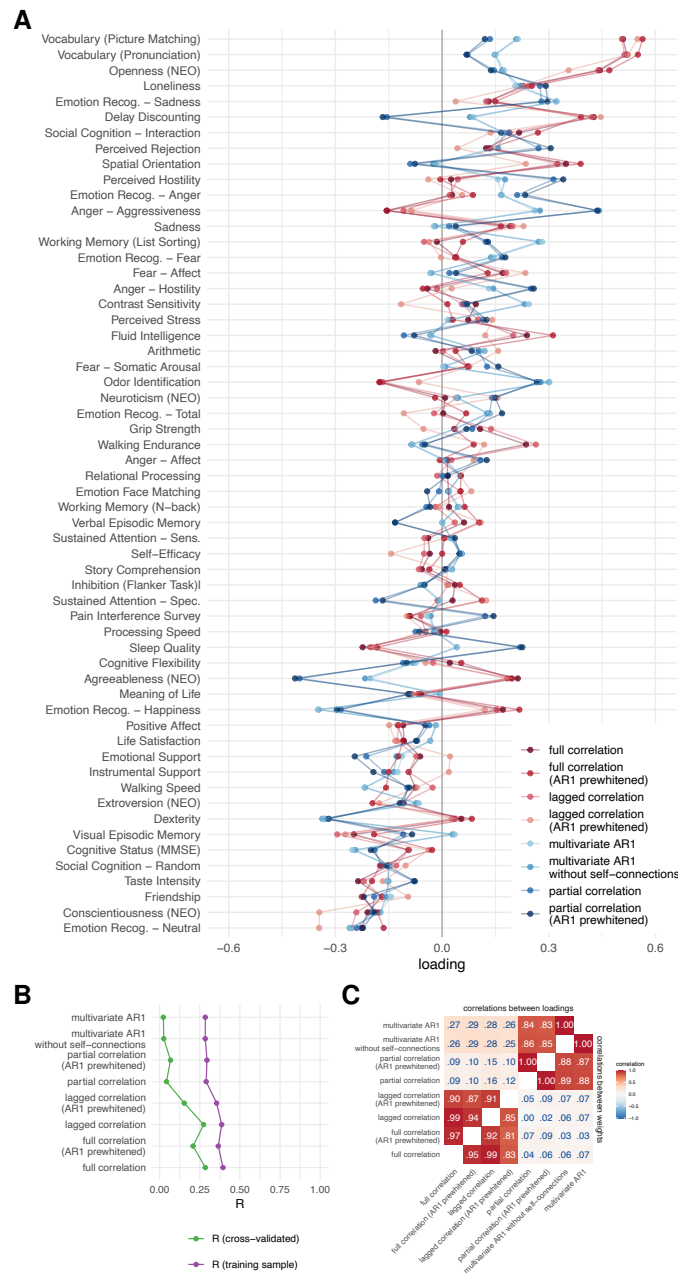


Figure 6: Results of canonical correlation analysis for brain-behavior associations. A. CCA loadings. B. First canonical correlation on test and training set, C. Correlations between canonical loadings and weights across functional connectivity methods for first canonical components.

354 conditions with high signal length.

355 4. Discussion

356 In this study, we addressed the question of whether the temporal order of the BOLD fMRI time series contains
 357 information important for the study of the fMRI brain functional connectivity. To this end, we compared FC estimates

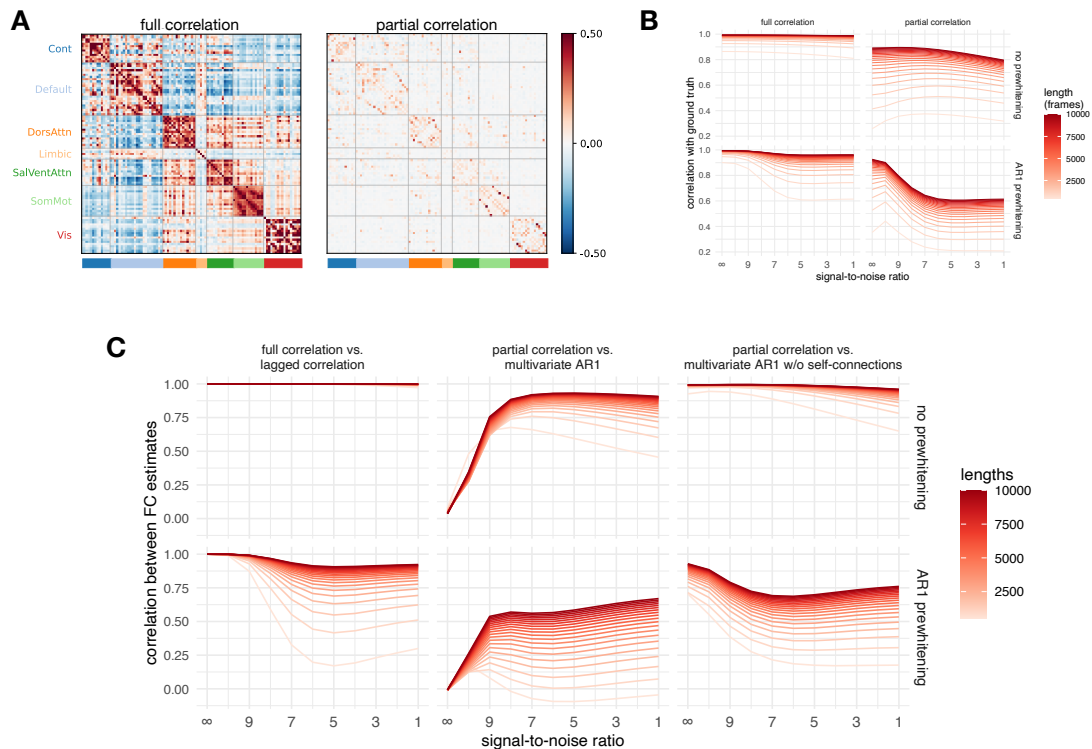


Figure 7: **Results of simulation.** **A.** Ground truth matrices (mean over participants). Note that all ground truth autoregressive model coefficients equal zero, since the simulated events were not autocorrelated. **B.** Correlation between the ground truth and the simulated data for all FC methods and their relationship to the noise level and signal length. **C.** Correlations between selected pairs of FC methods as a function of noise and signal length for simulated data. Note that the data in the second row related to multivariate AR models were not prewhitened before computation because the self-connections act as prewhitening.

358 between methods that differed in their sensitivity to temporal order, i.e., static and dynamic measures of FC. We also
 359 compared methods that differed in the number of variables considered in estimating the connectivity of individual
 360 edges, i.e., bivariate and multivariate. Our results suggest that dynamic FC connectivity methods provide similar con-
 361 nectivity estimates as static FC methods of the same type (bivariate or multivariate), whereas bivariate and multivariate
 362 methods differ in terms of the explanation of individual differences in behavior.

363 4.1. Dynamic functional connectomes represent information similar to static functional connectomes

364 By directly comparing the FC matrices, we have shown that the estimates of the dynamic FC represent information
 365 similar to the estimates of the static FC. The similarity between estimates of FC, obtained by different methods,
 366 depended on several factors. First, there were high correlations between the FC estimates when the same number of
 367 variables was considered.

368 Second, similarities between connectomes were greater when averages were compared at the group level than
 369 when correlations were aggregated across individual-level FC matrices. We believe that the differences between the
 370 group- and individual-level cases are mainly due to better SNR in the case of the group-level data. Two observations
 371 support this conclusion: first, similarities in FC estimates between methods were greater for participants with the
 372 highest data quality, and this effect was more pronounced when comparing individual-level matrices than at the group
 373 level. Second, edges with higher test-retest reliability (an indicator of SNR) were more similar between FC estimates
 374 obtained by different methods. Thus, we can conclude that SNR influences the similarity between FC estimates.

375 Using simulation, we tested the similarities between FC as a function of noise and signal length. We have shown
 376 that the dynamic FC estimates resemble static FC estimates even in the absence of true lagged correlation. The

377 similarity between the multivariate AR1 model and partial correlations can be partially explained by the fact that the
378 multivariate AR1 coefficients are a product of inverse covariance and lagged covariance matrix.

379 We also found a high similarity between the full and the lagged correlation. Therefore, the similarity between
380 the multivariate AR1 model and the partial correlation cannot be explained solely by the inclusion of the precision
381 matrix in the estimation of the coefficients of the multivariate AR model. Rather, the lagged covariance matrix also
382 contributes to this effect.

383 We hypothesized that the similarities between the dynamic and static FC estimates originate from autocorrelation
384 of the fMRI time series. We predicted that the similarities between the dynamic and static FC estimates would be at
385 least as large as the average autocorrelation of the fMRI time series and that this similarity would be reduced after
386 prewhitening. Both predictions were confirmed in experimental and simulated data. However, even when autocorre-
387 lation was reduced to virtually zero at all lags (this occurred at prewhitening order 3), similarities between estimates
388 based on dynamic and static FC models remained high for group-level matrices and simulated data. This suggests that
389 prewhitening (or even the presence of noise that reduces autocorrelation) does not completely eliminate the influence
390 of convolution with HRF on the estimation of dynamic FC.

391 We conclude that even if AR models represent information that goes beyond the static FC, this cannot be claimed
392 on the basis of a direct comparison of dynamic and static FC estimates. One of the main differences between static
393 and dynamic FC methods is the ability of dynamic FC methods to estimate the directionality of connections [7]. FC
394 matrices based on dynamic FC methods are therefore asymmetric. To allow comparisons between static and dynamic
395 FC matrices, the former were symmetrized and the information about the directionality of the connections was lost.
396 To test the possibility that there is specific information in the dynamic FC estimates that could not be detected in a
397 direct comparison of the FC matrices, we additionally compared the patterns of brain-behavior associations between
398 FC methods.

399 *4.2. Dynamic FC models do not explain additional variance in behavior over static FC models*

400 We used the variance component model (VCM) and canonical correlation analysis (CCA) to estimate brain-
401 behavior associations. The results of both methods showed that there were no large differences between the dynamic
402 and static FC estimates in the patterns of associations with behavior. However, we found large differences between
403 the bivariate and multivariate methods. These differences were specific to the method used to estimate brain-behavior
404 associations.

405 In the case of CCA, the canonical correlations were higher for bivariate methods than for multivariate methods.
406 The cross-validated canonical correlations were around 0 for multivariate methods, indicating that the results were not
407 generalizable. In contrast, the difference between the canonical correlations in the training and test sets was relatively
408 small for the bivariate methods.

409 In the case of VCM, the multivariate methods explained on average about 30 percentage points more variance in
410 behavior than the bivariate methods. To better understand this observation, we examined the impact of inter-subject
411 similarities on VCM results. To this end, we added random noise to the data, reducing the similarities between
412 subjects. Interestingly, full correlation and partial correlation explained more variance in behavior on average when
413 we added random noise to the data. This may sound counterintuitive, but keep in mind that VCM was developed
414 to estimate heritability [43], that is, the proportion of variance in phenotype that can be explained by variance in
415 genotype. Holding the environment constant, higher genetic similarity would reduce the estimate of heritability. If
416 all individuals within a sample had the same genotype, heritability would be zero because no variance in phenotype
417 could be explained by variance in genotype. The input to VCM is a between-subject similarity matrix (usually a
418 genetic similarity matrix or, in our case, a connectome similarity matrix). Participants were more similar when we
419 used full correlation as an estimate of FC compared to partial correlation. This explains the observation that the partial
420 correlation explained more variance in behavior.

421 Our second simulation showed that the partial correlation estimates are less stable and more affected by noise
422 and signal length. This explains the apparent discrepancy between VCM and CCA. Our results show that when we
423 add noise to the experimental data, participants become more dissimilar and, in the case of VCM, the proportion of
424 behavioral variance explained by the variance in the connectome becomes larger. In the case of CCA, lower SNR leads
425 to lower and less generalizable canonical correlations for multivariate FC methods. For this reason, we recommend
426 that great care be taken when estimating brain-behavior associations with measures that are sensitive to noise.

427 Liégeois et al. [16] have used VCM to compare brain-behavior associations between correlation and the multi-
428 variate AR model. They concluded that the dynamic FC explained variance in behavior beyond that explained by
429 static FC. We have shown that these results are confounded by the mixing of two orthogonal properties of the FC
430 methods: sensitivity to the temporal order of time points and the number of regions used to estimate a single edge.
431 The difference between the explanatory value of the multivariate AR model and the full correlation is better explained
432 by the difference between the multivariate and bivariate nature of the method than by the sensitivity to the temporal
433 order of the time points.

434 *4.3. Limitations and future directions*

435 A number of limitations should be considered in drawing conclusions from our study. First, in our simulation,
436 we generated noise using a multivariate normal distribution. We could have used more advanced noise modeling that
437 incorporated specific noise components such as drift, moving average, physiological noise, and system noise [54].
438 Unlike white noise, these noise sources are autocorrelated and therefore could affect the (dynamic) FC estimates. We
439 wanted to keep the model simple and interpretable. Even with the simplest noise model without autocorrelation in
440 neural time series, we showed that AR models can be affected by convolution of the neural signal with HRF and that
441 consequently the dynamic FC estimates resemble the static FC. However, more advanced noise modeling could be
442 used for a more realistic assessment of the sources of similarities between different FC methods.

443 Similarly, we used a very simple procedure, prewhitening, to reduce autocorrelation. Other methods could also
444 be used to reduce autocorrelation, such as advanced physiological modeling [55, 56] or deconvolution [57]. Decon-
445 volution can improve dynamic [10] and static FC estimates [57]. However, Seth et al. [11] have shown that sufficient
446 sampling rate is more important for valid dynamic FC estimates. Unlike fMRI, electrophysiological measurements
447 such as EEG and MEG have sufficient sampling rates and do not require deconvolution, so they could be used to study
448 the relationship between static and dynamic FC [58].

449 *4.4. Conclusions*

450 Our results show that the dynamic FC estimates represent information about connectivity that is broadly similar
451 to the static FC. Moreover, we have shown that the similarity between dynamic and static FC is due, at least in part,
452 to the convolution of neural time series with HRF. In contrast, we observed lower similarities in the patterns of FC
453 estimates between multivariate and bivariate methods. Multivariate methods were more sensitive to noise and CCA
454 models based on multivariate methods were less generalizable.

455 Although dynamic FC models are useful as a model for directed FC or for modeling the evolution of neural time
456 series over time [15], our results suggest that estimates of the functional connectome do not change when temporal
457 information is taken into account. Dynamic FC estimates also show no advantage or difference from static FC in terms
458 of brain-behavior associations.

459 **5. Data and code availability**

460 Raw data are available as part of the Human Connectome Project (<https://www.humanconnectome.org/>).
461 The function to compute the variance component model is available in the repository: [https://github.com/
462 RaphaelLiegeois/FC-Behavior](https://github.com/RaphaelLiegeois/FC-Behavior). For CCA, we used the GEMMR package: [https://github.com/murraylab/
463 gemmr](https://github.com/murraylab/gemmr). All other relevant functions are available on Open Science Framework: [https://dx.doi.org/10.17605/
464 OSF.IO/XFTDH](https://dx.doi.org/10.17605/OSF.IO/XFTDH).

465 **6. Author contributions**

466 **Andraž Matkovič:** Conceptualization, Methodology, Formal analysis, Investigation, Writing - Original Draft,
467 Writing - Review & Editing, Visualization. **Alan Anticevic:** Conceptualization, Writing - Review & Editing. **John
468 D. Murray:** Conceptualization, Writing - Review & Editing. **Grega Repovš:** Conceptualization, Software, Writing
469 - Original Draft, Writing - Review & Editing, Supervision, Project administration, Funding acquisition.

470 7. Competing Interests

471 J.D.M. and A.A. consult for and hold equity with Neumora (formerly BlackThorn Therapeutics), Manifest Tech-
472 nologies, and are co-inventors on the following patents: Anticevic A, Murray JD, Ji JL: Systems and Methods for
473 Neuro-Behavioral Relationships in Dimensional Geometric Embedding (N-BRIDGE), PCT International Application
474 No. PCT/US2119/022110, filed March 13, 2019 and Murray JD, Anticevic A, Martin, WJ:Methods and tools for
475 detecting, diagnosing, predicting, prognosticating, or treating a neurobehavioral phenotype in a subject, U.S. Appli-
476 cation No. 16/149,903 filed on October 2, 2018, U.S. Application for PCT International Application No. 18/054,009
477 filed on October 2, 2018. G.R. consults for and holds equity with Neumora (formerly BlackThorn Therapeutics) and
478 Manifest Technologies. A.M. declares no conflict of interest.

479 8. Funding sources

480 This work was supported by the Slovenian Research Agency grants J7-8275, P3-0338, P5-0110.

481 9. Acknowledgments

482 Data were provided by the Human Connectome Project, WU-Minn Consortium (Principal Investigators: David
483 Van Essen and Kamil Ugurbil; 1U54MH091657) funded by the 16 NIH Institutes and Centers that support the NIH
484 Blueprint for Neuroscience Research; and by the McDonnell Center for Systems Neuroscience at Washington Uni-
485 versity.

486 10. Appendix

487 10.1. Motion scrubbing

488 Motion scrubbing is usually performed by removing bad frames before calculating the correlation or related mea-
489 sure of static FC. This is not appropriate in the case of dynamic FC or autocorrelation, since removing time points
490 disrupts the autocorrelation structure of time series.

491 To overcome this limitation, a frame was considered bad if it was bad in either original or lagged time series.
492 Frames at transition between concatenated time series (last frame in the first time series and first frame in the next
493 time series) were also marked as bad in this case.

494 In the case of autoregressive models, transitions between runs (last frame of the previous run, first frame of the
495 next run) were excluded in the same manner as bad frames.

496 References

- 497 [1] A. Fornito, A. Zalesky, E. T. Bullmore, Fundamentals of Brain Network Analysis, Elsevier/Academic Press, Amsterdam ; Boston, 2016.
498 [2] A. T. Reid, D. B. Headley, R. D. Mill, R. Sanchez-Romero, L. Q. Uddin, D. Marinazzo, D. J. Lurie, P. A. Valdés-Sosa, S. J. Hanson,
499 B. B. Biswal, V. Calhoun, R. A. Poldrack, M. W. Cole, Advancing functional connectivity research from association to causation, Nature
500 Neuroscience 22 (2019) 1751–1760. doi:10.1038/s41593-019-0510-4.
501 [3] C. Wu, F. Ferreira, M. Fox, N. Harel, J. Hattangadi-Gluth, A. Horn, S. Jbabdi, J. Kahan, A. Oswal, S. A. Sheth, Y. Tie, V. Vakharia, L. Zrinzo,
502 H. Akram, Clinical applications of magnetic resonance imaging based functional and structural connectivity, NeuroImage 244 (2021) 118649.
503 doi:10.1016/j.neuroimage.2021.118649.
504 [4] S. H. Tompson, E. B. Falk, J. M. Vettel, D. S. Bassett, Network Approaches to Understand Individual Differences in Brain Connectivity:
505 Opportunities for Personality Neuroscience, Personality Neuroscience 1 (2018) e5. doi:10.1017/pen.2018.4.
506 [5] M. W. Cole, T. Ito, D. S. Bassett, D. H. Schultz, Activity flow over resting-state networks shapes cognitive task activations, Nature
507 Neuroscience 19 (2016) 1718–1726. doi:10.1038/nn.4406.
508 [6] T. A. W. Bolton, R. Liegeois, The arrow-of-time in neuroimaging time series identifies causal triggers of brain function, 2022. doi:10.1101/
509 2022.05.11.491521.
510 [7] S. M. Smith, K. L. Miller, G. Salimi-Khorshidi, M. Webster, C. F. Beckmann, T. E. Nichols, J. D. Ramsey, M. W. Woolrich, Network
511 modelling methods for fMRI, NeuroImage 54 (2011) 875–891. doi:10.1016/j.neuroimage.2010.08.063.
512 [8] K. Friston, Causal Modelling and Brain Connectivity in Functional Magnetic Resonance Imaging, PLoS Biology 7 (2009) e1000033.
513 doi:10.1371/journal.pbio.1000033.
514 [9] K. Friston, Dynamic causal modeling and Granger causality Comments on: The identification of interacting networks in the brain using
515 fMRI: Model selection, causality and deconvolution, NeuroImage 58 (2011) 303–305. doi:10.1016/j.neuroimage.2009.09.031.

- 516 [10] O. David, I. Guillemain, S. Saittel, S. Reyt, C. Deransart, C. Segebarth, A. Depaulis, Identifying Neural Drivers with Functional MRI: An
517 Electrophysiological Validation, *PLoS Biology* 6 (2008) e315. doi:10.1371/journal.pbio.0060315.
- 518 [11] A. K. Seth, P. Chorley, L. C. Barnett, Granger causality analysis of fMRI BOLD signals is invariant to hemodynamic convolution but not
519 downsampling, *NeuroImage* 65 (2013) 540–555. doi:10.1016/j.neuroimage.2012.09.049.
- 520 [12] V. Pallarés, A. Insabato, A. Sanjuán, S. Kühn, D. Mantini, G. Deco, M. Gilson, Extracting orthogonal subject- and condition-specific
521 signatures from fMRI data using whole-brain effective connectivity, *NeuroImage* 178 (2018) 238–254. doi:10.1016/j.neuroimage.
522 2018.04.070.
- 523 [13] M. Gilson, G. Deco, K. J. Friston, P. Hagmann, D. Mantini, V. Betti, G. L. Romani, M. Corbetta, Effective connectivity inferred from fMRI
524 transition dynamics during movie viewing points to a balanced reconfiguration of cortical interactions, *NeuroImage* 180 (2018) 534–546.
525 doi:10.1016/j.neuroimage.2017.09.061.
- 526 [14] M. Gilson, R. Moreno-Bote, A. Ponce-Alvarez, P. Ritter, G. Deco, Estimation of Directed Effective Connectivity from fMRI Functional
527 Connectivity Hints at Asymmetries of Cortical Connectome, *PLOS Computational Biology* 12 (2016) e1004762. doi:10.1371/journal.
528 pcbi.1004762.
- 529 [15] R. Liégeois, T. O. Laumann, A. Z. Snyder, J. Zhou, B. T. Yeo, Interpreting temporal fluctuations in resting-state functional connectivity MRI,
530 *NeuroImage* 163 (2017) 437–455. doi:10/gcsbkz.
- 531 [16] R. Liégeois, J. Li, R. Kong, C. Orban, D. Van De Ville, T. Ge, M. R. Sabuncu, B. T. T. Yeo, Resting brain dynamics at different timescales
532 capture distinct aspects of human behavior, *Nature Communications* 10 (2019) 2317. doi:10/gf3k2q.
- 533 [17] M. R. Arbabshirani, A. Preda, J. G. Vaidya, S. G. Potkin, G. Pearlson, J. Voyvodic, D. Mathalon, T. van Erp, A. Michael, K. A. Kiehl, J. A.
534 Turner, V. D. Calhoun, Autoconnectivity: A new perspective on human brain function, *Journal of Neuroscience Methods* 323 (2019) 68–76.
535 doi:10/gf2tvj.
- 536 [18] R. Liégeois, A. Santos, V. Matta, D. Van De Ville, A. H. Sayed, Revisiting correlation-based functional connectivity and its relationship with
537 structural connectivity, *Network Neuroscience* 4 (2020) 1235–1251. doi:10/gm79q6.
- 538 [19] H. Honari, A. S. Choe, J. J. Pekar, M. A. Lindquist, Investigating the impact of autocorrelation on time-varying connectivity, *NeuroImage*
539 197 (2019) 37–48. doi:10/gm7955.
- 540 [20] L. Novelli, J. T. Lizier, Inferring network properties from time series using transfer entropy and mutual information: Validation of multivariate
541 versus bivariate approaches, *Network Neuroscience* (2021) 1–32. doi:10.1162/netn_a_00178.
- 542 [21] W. Cheng, X. Ji, J. Zhang, J. Feng, Individual classification of ADHD patients by integrating multiscale neuroimaging markers and advanced
543 pattern recognition techniques, *Frontiers in Systems Neuroscience* 6 (2012). doi:10.3389/fnsys.2012.00058.
- 544 [22] H. Cai, J. Zhu, Y. Yu, Robust prediction of individual personality from brain functional connectome, *Social Cognitive and Affective*
545 *Neuroscience* 15 (2020) 359–369. doi:10.1093/scan/nsaa044.
- 546 [23] A. Abraham, M. P. Milham, A. Di Martino, R. C. Craddock, D. Samaras, B. Thirion, G. Varoquaux, Deriving reproducible biomarkers from
547 multi-site resting-state data: An Autism-based example, *NeuroImage* 147 (2017) 736–745. doi:10.1016/j.neuroimage.2016.10.045.
- 548 [24] K. Dadi, M. Rahim, A. Abraham, D. Chyzyk, M. Milham, B. Thirion, G. Varoquaux, Benchmarking functional connectome-based predictive
549 models for resting-state fMRI, *NeuroImage* 192 (2019) 115–134. doi:10.1016/j.neuroimage.2019.02.062.
- 550 [25] D. C. Van Essen, S. M. Smith, D. M. Barch, T. E. Behrens, E. Yacoub, K. Ugurbil, The WU-Minn Human Connectome Project: An overview,
551 *NeuroImage* 80 (2013) 62–79. doi:10/f46ktq.
- 552 [26] M. F. Glasser, S. N. Sotiropoulos, J. A. Wilson, T. S. Coalson, B. Fischl, J. L. Andersson, J. Xu, S. Jbabdi, M. Webster, J. R. Polimeni,
553 D. C. Van Essen, M. Jenkinson, The minimal preprocessing pipelines for the Human Connectome Project, *NeuroImage* 80 (2013) 105–124.
554 doi:10/f46nj4.
- 555 [27] G. Salimi-Khorshidi, G. Douaud, C. F. Beckmann, M. F. Glasser, L. Griffanti, S. M. Smith, Automatic denoising of functional MRI data:
556 Combining independent component analysis and hierarchical fusion of classifiers, *NeuroImage* 90 (2014) 449–468. doi:10/ggwbj.
- 557 [28] M. F. Glasser, T. S. Coalson, E. C. Robinson, C. D. Hacker, J. Harwell, E. Yacoub, K. Ugurbil, J. Andersson, C. F. Beckmann, M. Jenkinson,
558 S. M. Smith, D. C. Van Essen, A multi-modal parcellation of human cerebral cortex, *Nature* 536 (2016) 171–178. doi:10/f8z3gb.
- 559 [29] J. L. Ji, J. Demšar, C. Fonteneau, Z. Tamayo, L. Pan, A. Kraljic, A. Matkovic, M. Helmer, S. Warrington, M. Harms, S. N. Sotiropoulos,
560 J. D. Murray, G. Repovš, QuNex – An Integrative Platform for Reproducible Neuroimaging Analytics, *bioRxiv* (2022) 16. doi:10.1101/
561 2022.06.03.494750.
- 562 [30] M. R. Arbabshirani, E. Damaraju, R. Phlypo, S. Plis, E. Allen, S. Ma, D. Mathalon, A. Preda, J. G. Vaidya, T. Adali, V. D. Calhoun, Impact
563 of autocorrelation on functional connectivity, *NeuroImage* 102 (2014) 294–308. doi:10/f6rcdt.
- 564 [31] C. E. Davey, D. B. Grayden, G. F. Egan, L. A. Johnston, Filtering induces correlation in fMRI resting state data, *NeuroImage* 64 (2013)
565 728–740. doi:10/f4jgxv.
- 566 [32] U. Pervaiz, D. Vidaurre, M. W. Woolrich, S. M. Smith, Optimising network modelling methods for fMRI, *NeuroImage* 211 (2020) 116604.
567 doi:10/ggx68f.
- 568 [33] C. Chatfield, H. Xing, *The Analysis of Time Series: An Introduction with R*, Chapman & Hall/CRC Texts in Statistical Science Series,
569 seventh edition ed., CRC Press, Taylor & Francis Group, Boca Raton, 2019.
- 570 [34] J. Friedman, T. Hastie, R. Tibshirani, Regularization Paths for Generalized Linear Models via Coordinate Descent, *Journal of Statistical*
571 *Software* 33 (2010). doi:10.18637/jss.v033.i01.
- 572 [35] C.-M. Ting, A.-K. Seghouane, M. U. Khalid, S.-H. Salleh, Is First-Order Vector Autoregressive Model Optimal for fMRI Data?, *Neural*
573 *Computation* 27 (2015) 1857–1871. doi:10/f7n8qq.
- 574 [36] P. A. Valdes-Sosa, Spatio-Temporal Autoregressive Models Defined Over Brain Manifolds, *Neuroinformatics* 2 (2004) 239–250. doi:10/
575 fs5xbw.
- 576 [37] J. Casorso, X. Kong, W. Chi, D. Van De Ville, B. T. Yeo, R. Liégeois, Dynamic mode decomposition of resting-state and task fMRI,
577 *NeuroImage* 194 (2019) 42–54. doi:10/gfx53r.
- 578 [38] D. Bates, M. Mächler, B. Bolker, S. Walker, Fitting Linear Mixed-Effects Models Using **lme4**, *Journal of Statistical Software* 67 (2015).
579 doi:10/gcrnkw.
- 580 [39] E. Jolly, Pymer4: Connecting R and Python for Linear Mixed Modeling, *Journal of Open Source Software* 3 (2018) 862. doi:10/gnzgqv.

- 581 [40] L. Li, L. Zeng, Z.-J. Lin, M. Cazzell, H. Liu, Tutorial on use of intraclass correlation coefficients for assessing intertest reliability and its
582 application in functional near-infrared spectroscopy-based brain imaging, *Journal of Biomedical Optics* 20 (2015) 050801. doi:10/gj7s8x.
- 583 [41] J. Li, R. Kong, R. Liégeois, C. Orban, Y. Tan, N. Sun, A. J. Holmes, M. R. Sabuncu, T. Ge, B. T. Yeo, Global signal regression strengthens
584 association between resting-state functional connectivity and behavior, *NeuroImage* 196 (2019) 126–141. doi:10/gj8p69.
- 585 [42] R. Kashyap, R. Kong, S. Bhattacharjee, J. Li, J. Zhou, B. Thomas Yeo, Individual-specific fMRI-Subspaces improve functional connectivity
586 prediction of behavior, *NeuroImage* 189 (2019) 804–812. doi:10/gft3tt.
- 587 [43] T. Ge, M. Reuter, A. M. Winkler, A. J. Holmes, P. H. Lee, L. S. Tirrell, J. L. Roffman, R. L. Buckner, J. W. Smoller, M. R. Sabuncu,
588 Multidimensional heritability analysis of neuroanatomical shape, *Nature Communications* 7 (2016) 13291. doi:10/f9b8cv.
- 589 [44] D. J. Stekhoven, P. Bühlmann, MissForest—non-parametric missing value imputation for mixed-type data, *Bioinformatics* 28 (2012) 112–118.
590 doi:10/dhxth8.
- 591 [45] T. Ge, T. E. Nichols, P. H. Lee, A. J. Holmes, J. L. Roffman, R. L. Buckner, M. R. Sabuncu, J. W. Smoller, Massively expedited genome-wide
592 heritability analysis (MEGHA), *Proceedings of the National Academy of Sciences* 112 (2015) 2479–2484. doi:10/f63g67.
- 593 [46] A. C. Rencher, *Methods of Multivariate Analysis*, Wiley Series in Probability and Mathematical Statistics, 2nd ed ed., J. Wiley, New York,
594 2002.
- 595 [47] M. Helmer, S. Warrington, A.-R. Mohammadi-Nejad, J. L. Ji, A. Howell, B. Rosand, A. Anticevic, S. N. Sotiropoulos, J. D. Murray, On
596 stability of Canonical Correlation Analysis and Partial Least Squares with application to brain-behavior associations, 2020. doi:10.1101/
597 2020.08.25.265546.
- 598 [48] A. M. Winkler, O. Renaud, S. M. Smith, T. E. Nichols, Permutation inference for canonical correlation analysis, *NeuroImage* 220 (2020)
599 117065. doi:10.1016/j.neuroimage.2020.117065.
- 600 [49] H.-T. Wang, J. Smallwood, J. Mourao-Miranda, C. H. Xia, T. D. Satterthwaite, D. S. Bassett, D. Bzdok, Finding the needle in a high-
601 dimensional haystack: Canonical correlation analysis for neuroscientists, *NeuroImage* 216 (2020) 116745. doi:10.1016/j.neuroimage.
602 2020.116745.
- 603 [50] X. Zhuang, Z. Yang, D. Cordes, A technical review of canonical correlation analysis for neuroscience applications, *Human Brain Mapping*
604 41 (2020) 3807–3833. doi:10.1002/hbm.25090.
- 605 [51] S. M. Smith, T. E. Nichols, D. Vidaurre, A. M. Winkler, T. E. J. Behrens, M. F. Glasser, K. Ugurbil, D. M. Barch, D. C. Van Essen, K. L.
606 Miller, A positive-negative mode of population covariation links brain connectivity, demographics and behavior, *Nature Neuroscience* 18
607 (2015) 1565–1567. doi:10.1038/nn.4125.
- 608 [52] A. Schaefer, R. Kong, E. M. Gordon, T. O. Laumann, X.-N. Zuo, A. J. Holmes, S. B. Eickhoff, B. T. T. Yeo, Local-Global Parcellation of the
609 Human Cerebral Cortex from Intrinsic Functional Connectivity MRI, *Cerebral Cortex* 28 (2018) 3095–3114. doi:10/gd738m.
- 610 [53] E. B. Erhardt, E. A. Allen, Y. Wei, T. Eichele, V. D. Calhoun, SimTB, a simulation toolbox for fMRI data under a model of spatiotemporal
611 separability, *NeuroImage* 59 (2012) 4160–4167. doi:10/cr4g9g.
- 612 [54] C. T. Ellis, C. Baldassano, A. C. Schapiro, M. B. Cai, J. D. Cohen, Facilitating open-science with realistic fMRI simulation: Validation and
613 application, *PeerJ* 8 (2020) e8564. doi:10/ght935.
- 614 [55] J. E. Chen, J. R. Polimeni, S. Bollmann, G. H. Glover, On the analysis of rapidly sampled fMRI data, *NeuroImage* 188 (2019) 807–820.
615 doi:10/gfvhhv.
- 616 [56] S. Bollmann, A. M. Puckett, R. Cunnington, M. Barth, Serial correlations in single-subject fMRI with sub-second TR, *NeuroImage* 166
617 (2018) 152–166. doi:10/gcr9cx.
- 618 [57] D. Rangaprakash, G.-R. Wu, D. Marinazzo, X. Hu, G. Deshpande, Hemodynamic response function (HRF) variability confounds resting-state
619 fMRI functional connectivity, *Magnetic Resonance in Medicine* 80 (2018) 1697–1713. doi:10/gkzm4c.
- 620 [58] E. Tagliazucchi, H. Laufs, Multimodal Imaging of Dynamic Functional Connectivity, *Frontiers in Neurology* 6 (2015). doi:10.3389/fneur.
621 2015.00010.

622 **11. Supplement**

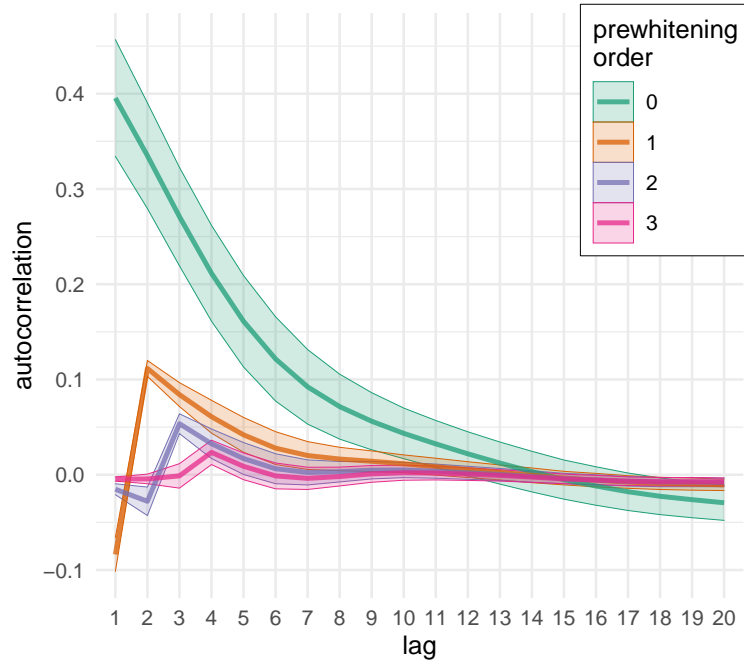


Figure S1: **Autocorrelation function of experimental data as a function of prewhitening order.** The mean autocorrelation function was computed over all participants and regions; the ribbons represent the standard deviation. Prewhitening drastically reduced autocorrelation even at low orders. Interestingly, prewhitening at orders 1 and 2 reversed the sign of autocorrelation in low lags.

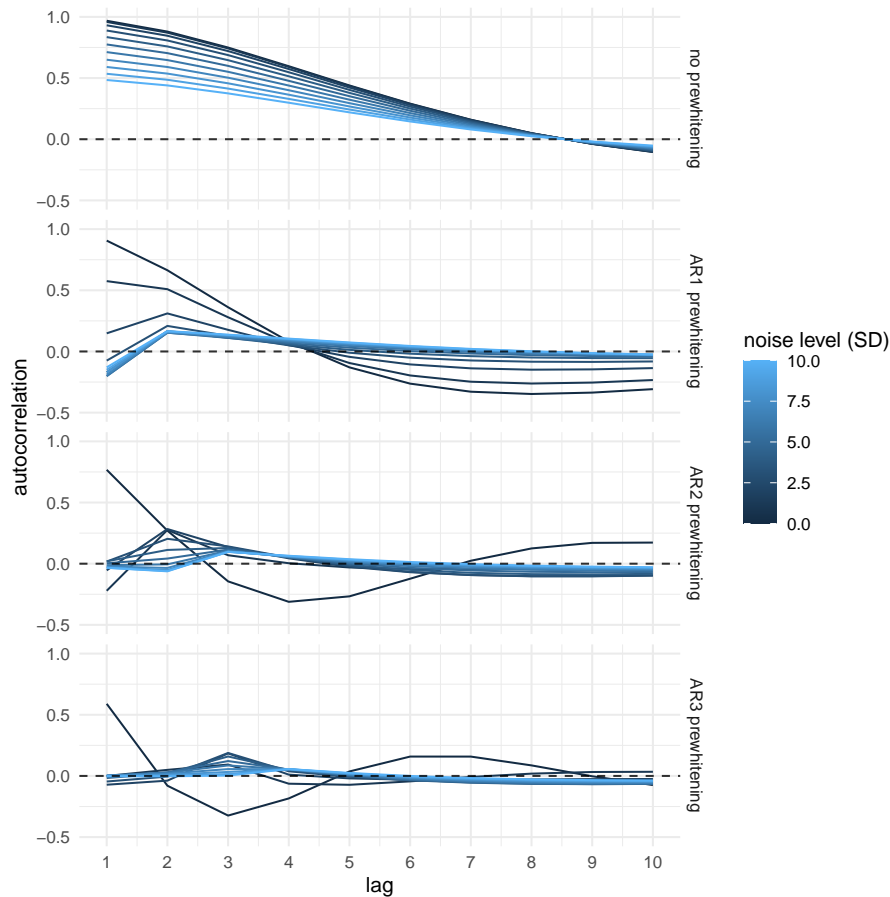


Figure S2: **The autocorrelation function of simulated data as a function of prewhitening order and noise.** The mean autocorrelation function was computed over all participants and regions. In general, noise and prewhitening reduced absolute autocorrelation. The shape of the autocorrelation function varied as a function of noise and prewhitening. In case without prewhitening, autocorrelation monotonically decreased and reached 0 at lag 8. After prewhitening, autocorrelation varied between positive and negative values, and this was most pronounced in cases without noise. The autocorrelation function was more similar to the experimental data in cases with low levels of noise.

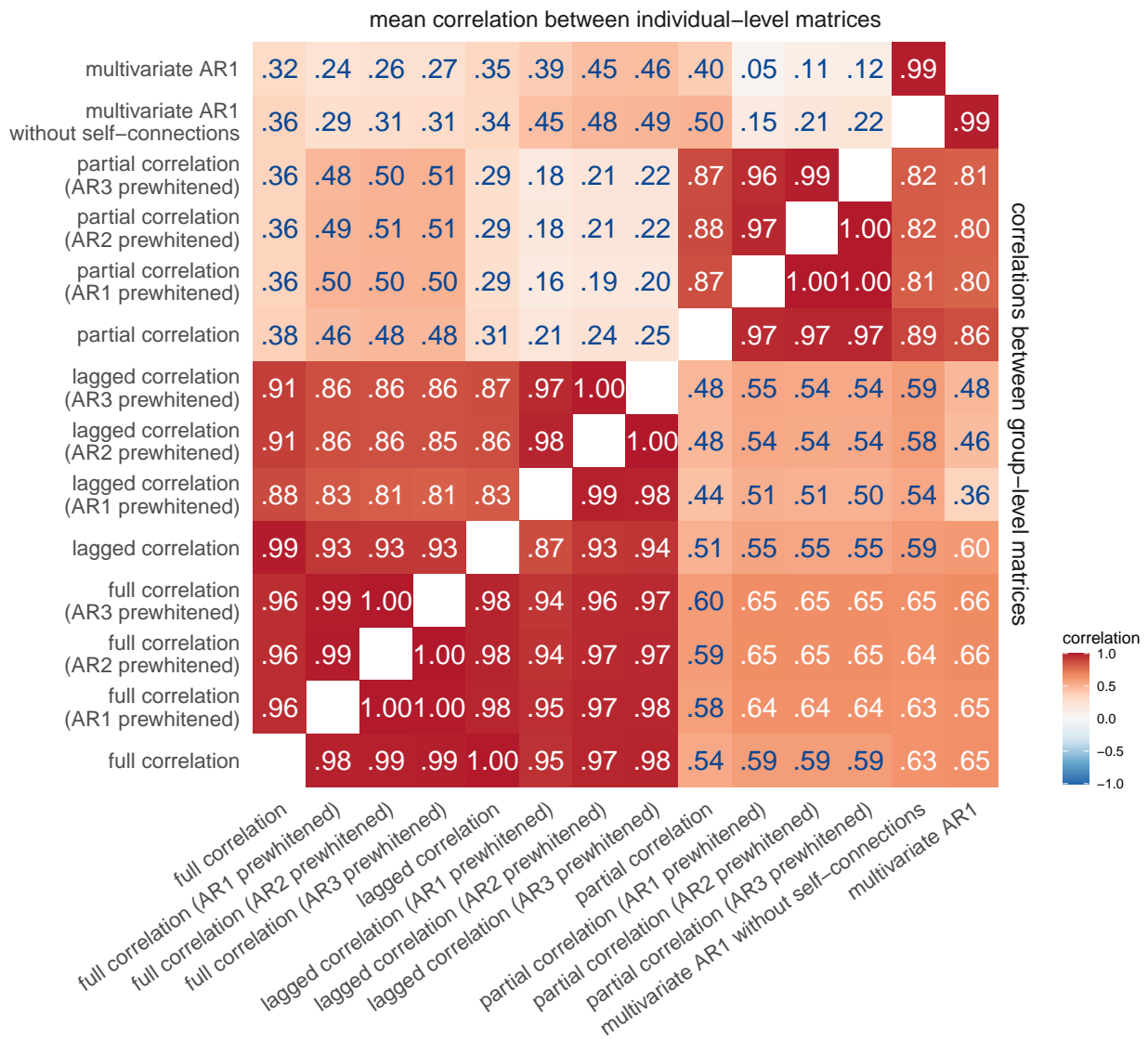


Figure S3: **Correlations between connectivity methods.** Same as in Figure 2 but includes all orders of prewhitening.

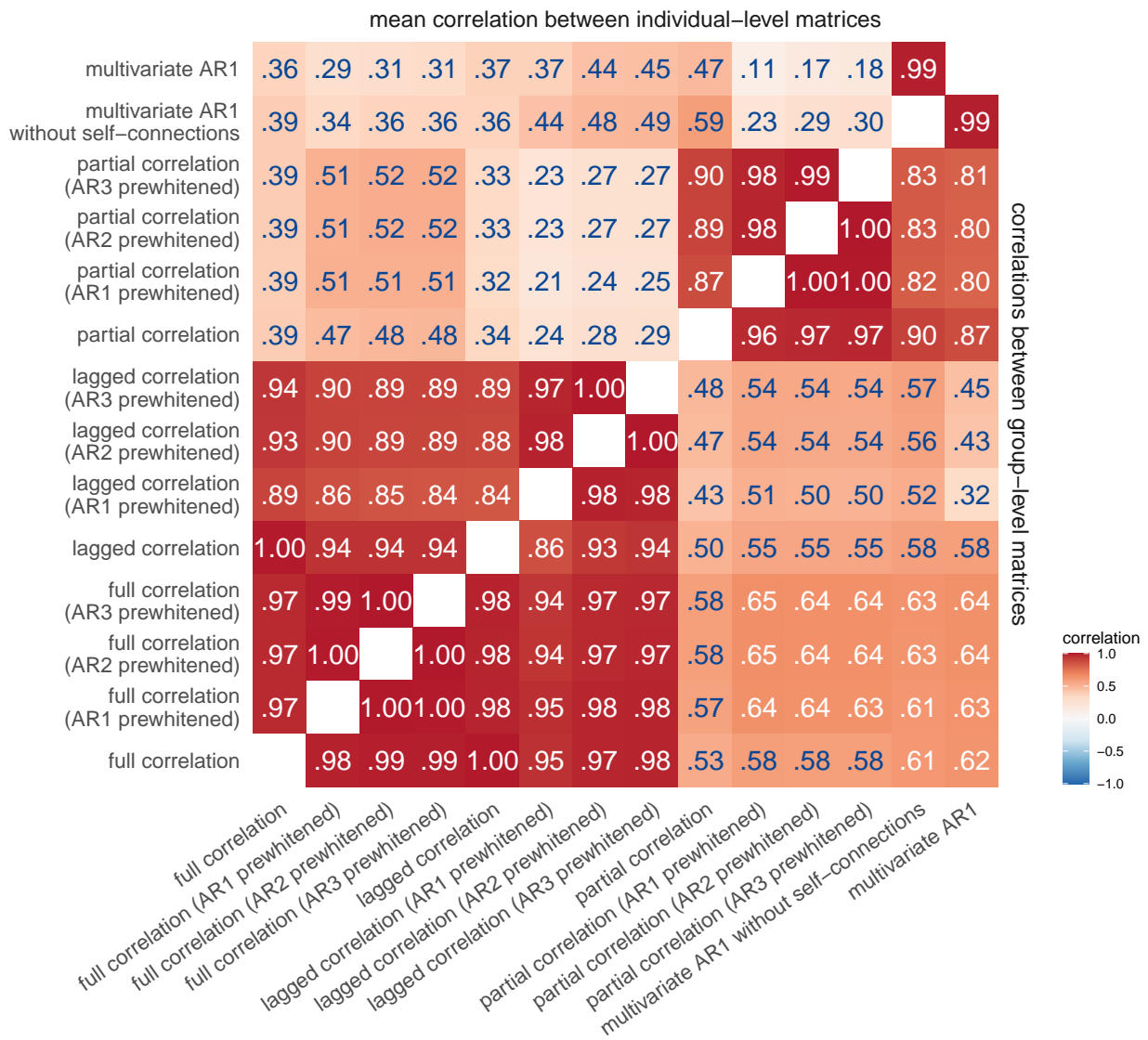


Figure S4: Correlations between connectivity methods on 200 participants with highest quality data.

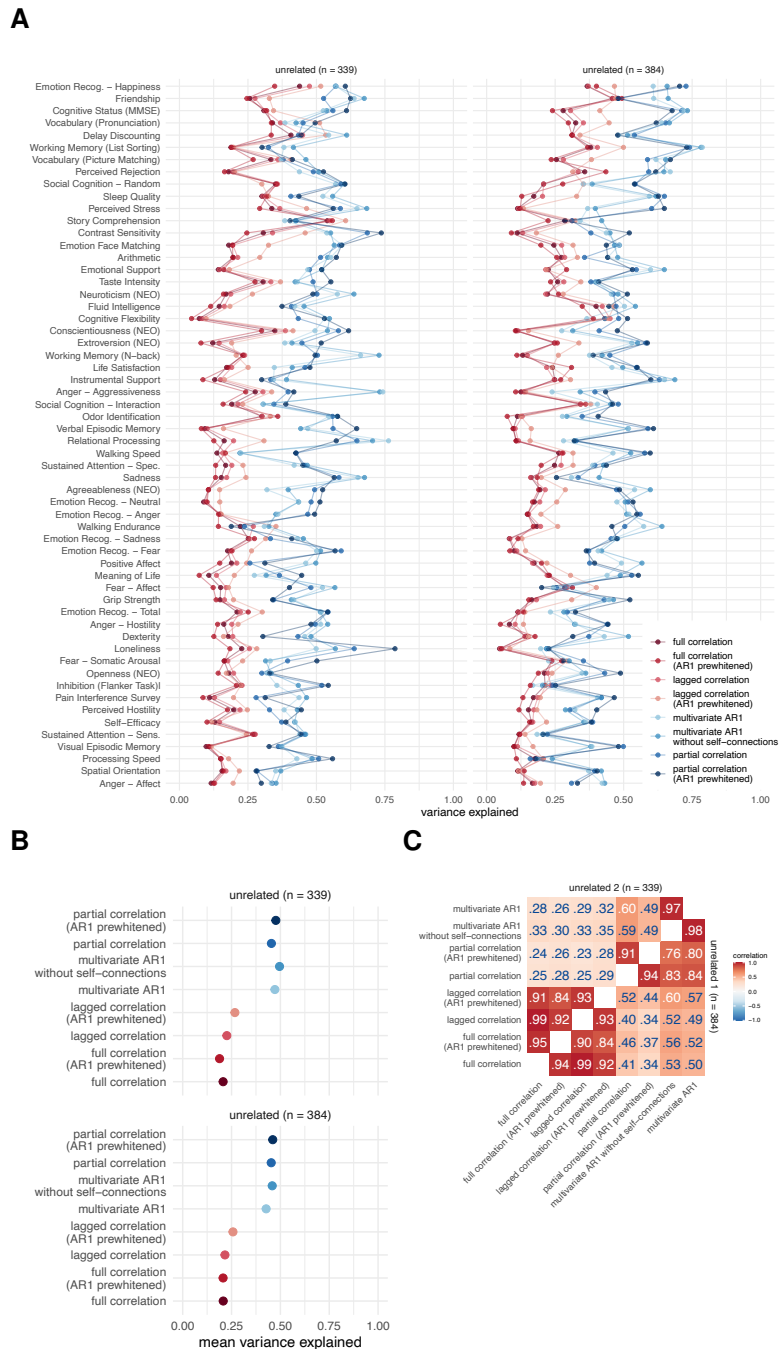


Figure S5: Results of variance component model for brain-behavior associations on subsamples of unrelated participants. (A) Variance explained for individual traits estimated with different connectivity methods, (B) mean variance explained, and (C) similarities of explained variance patterns between connectivity methods. The traits are ordered according to the mean variance explained across connectivity methods. The same as in Figure 4 but in subsamples of unrelated participants.

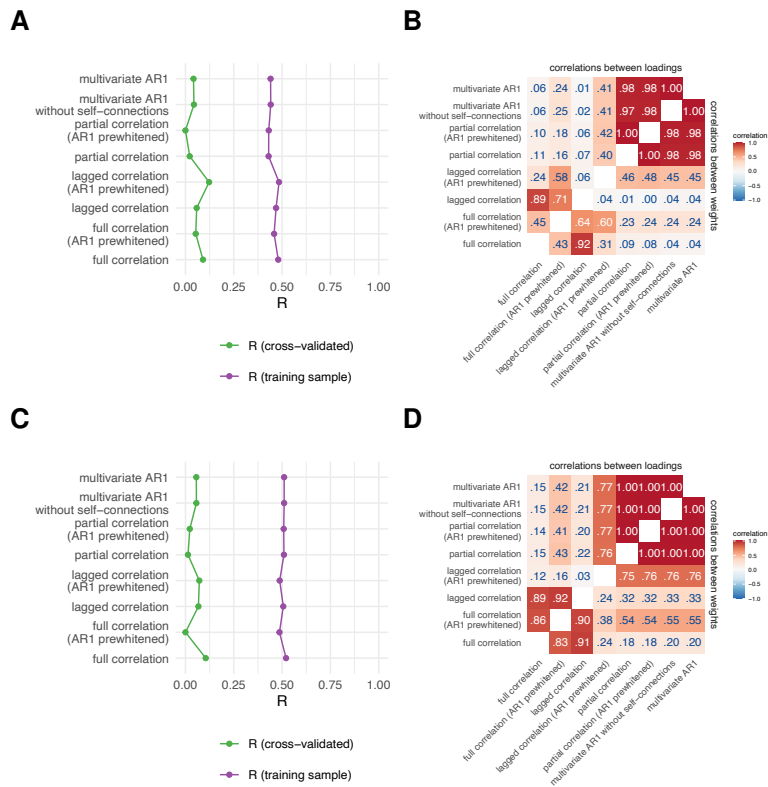


Figure S6: **Results of canonical correlation analysis for brain-behavior associations on subsamples of unrelated participants.** (A,C) First canonical correlation on test and training set in the first (A, $n = 384$) and second subsample (C, $n = 339$). (B,D) Correlations between canonical loadings and weights across FC methods for the first canonical components on the first (B) and second (D) subsample.

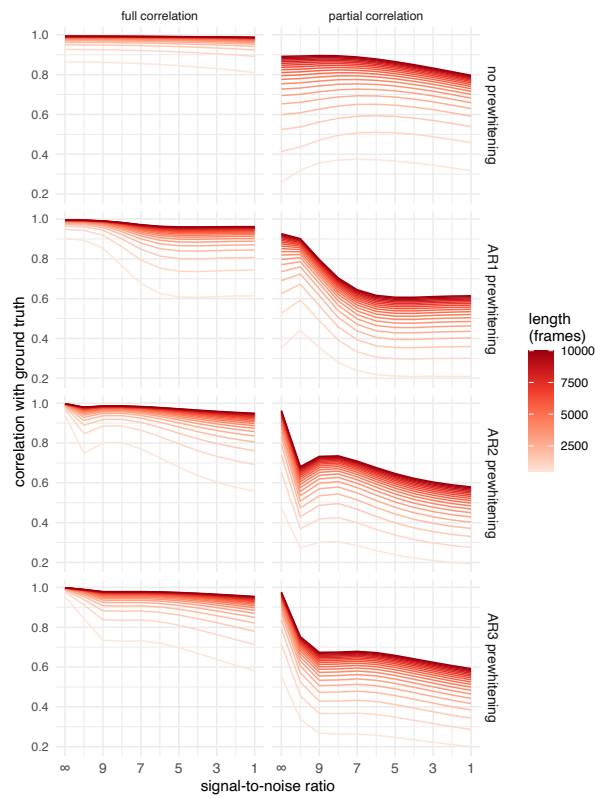


Figure S7: **Correlation between ground truth and simulated data for all FC methods in association with noise and signal length.** Same as in Figure 7B but includes all orders of prewhitening.

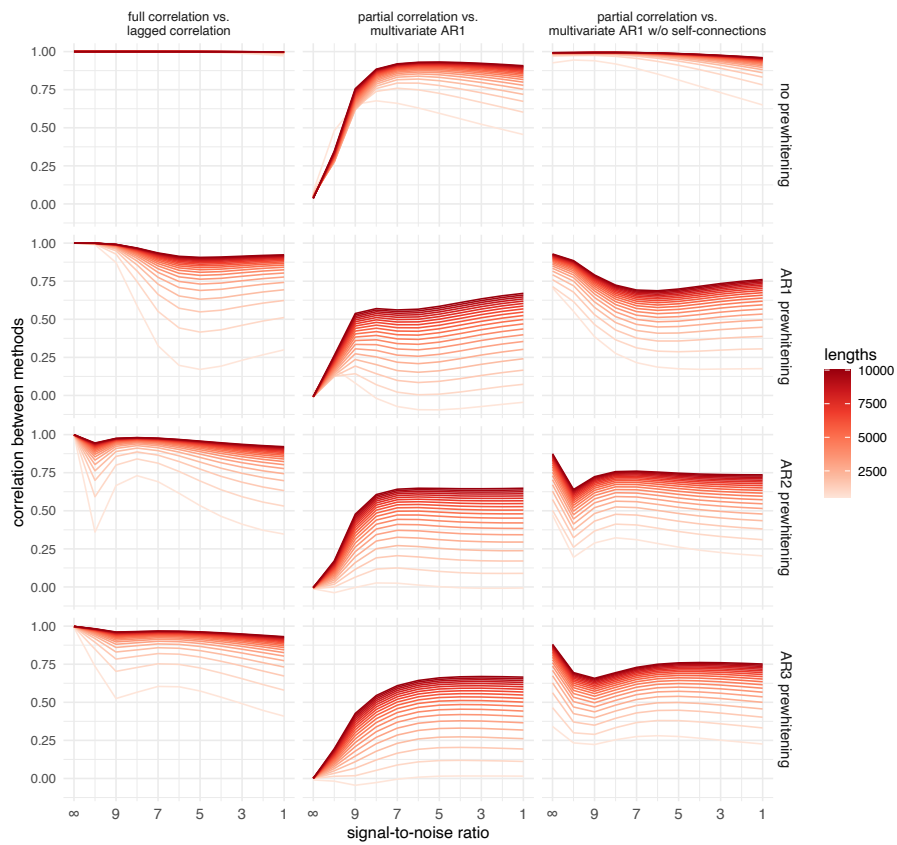


Figure S8: Correlation between selected pairs of FC methods as a function of noise and signal length on simulated data. Same as in Figure 7C but includes all prewhitening orders.

HCP Field	Friendly Name	HCP Field	Friendly Name
PicSeq_Unadj	Visual Episodic Memory	WM_Task_Acc	Working Memory (N-back)
CardSort_Unadj	Cognitive Flexibility	NEOFAC_A	Agreeableness (NEO)
Flanker_Unadj	Inhibition (Flanker Task)	NEOFAC_O	Openness (NEO)
PMAT24_A_CR	Fluid Intelligence	NEOFAC_C	Conscientiousness (NEO)
ReadEng_Unadj	Vocabulary (Pronunciation)	NEOFAC_N	Neuroticism (NEO)
PicVocab_Unadj	Vocabulary (Picture Matching)	NEOFAC_E	Extroversion (NEO)
ProcSpeed_Unadj	Processing Speed	ER40_CR	Emotion Recog. - Total
DDisc_AUC_40K	Delay Discounting	ER40ANG	Emotion Recog. - Anger
VSPLIT_TC	Spatial Orientation	ER40FEAR	Emotion Recog. - Fear
SCPT_SEN	Sustained Attention - Sens.	ER40HAP	Emotion Recog. - Happiness
SCPT_SPEC	Sustained Attention - Spec.	ER40NOE	Emotion Recog. - Neutral
IWRD_TOT	Verbal Episodic Memory	ER40SAD	Emotion Recog. - Sadness
ListSort_Unadj	Working Memory (List Sorting)	AngAffect_Unadj	Anger - Affect
MMSE_Score	Cognitive Status (MMSE)	AngHostil_Unadj	Anger - Hostility
PSQI_Score	Sleep Quality	AngAggr_Unadj	Anger - Aggressiveness
Endurance_Unadj	Walking Endurance	FearAffect_Unadj	Fear - Affect
GaitSpeed_Comp	Walking Speed	FearSomat_Unadj	Fear - Somatic Arousal
Dexterity_Unadj	Dexterity	Sadness_Unadj	Sadness
Strength_Unadj	Grip Strength	LifeSatisf_Unadj	Life Satisfaction
Odor_Unadj	Odor Identification	MeanPurp_Unadj	Meaning of Life
PainInterf_Tscore	Pain Interference Survey	PosAffect_Unadj	Positive Affect
Taste_Unadj	Taste Intensity	Friendship_Unadj	Friendship
Mars_Final	Contrast Sensitivity	Loneliness_Unadj	Loneliness
Emotion_Task_Face_Acc	Emotion Face Matching	PercHostil_Unadj	Perceived Hostility
Language_Task_Math_Avg_Difficulty_Level	Arithmetic	PercReject_Unadj	Perceived Rejection
Language_Task_Story_Avg_Difficulty_Level	Story Comprehension	EmotSupp_Unadj	Emotional Support
Relational_Task_Acc	Relational Processing	InstruSupp_Unadj	Instrumental Support
Social_Task_Perc_Random	Social Cognition - Random	PercStress_Unadj	Perceived Stress
Social_Task_Perc_TOM	Social Cognition - Interaction	SelfEff_Unadj	Self-Efficacy

Table S1: Behavioral measures.